Final Report

Performance Evaluation of an MM5 Simulation of May 29-July 3, 2006

Prepared for

Texas Commission on Environmental Quality
12118 Park 35 Circle
Austin, Texas 78753

Prepared by

Susan Kemball-Cook
Yiqin Jia
Ed Tai
Greg Yarwood

ENVIRON International Corporation
101 Rowland Way, Suite 220
Novato, CA 94945

August 31, 2007

TABLE OF CONTENTS

Page

EXECUTIVE SUMMARY ES-1

1. INTRODUCTION..... 1-1

2. MM5 CONFIGURATION 2-1

3. MODEL EVALUATION APPROACH..... 3-1

4. PRECIPITATION EVALUATION 4-1

5. EVALUATION OF PRESENCE OF ANOMALOUS CONVECTION 5-1

6. SUMMARY 6-1

REFERENCES..... R-1

TABLES

Table 2-1. MM5 vertical layer structure 2-2
Table 2-2. Physics options in the TCEQ and ENVIRON MM5 simulations..... 2-3
Table 2-3. Coefficients for observation nudging..... 2-4
Table 2-4. Coefficients for grid analysis nudging..... 2-4
Table 3-1. Statistical benchmarks for evaluating meteorological model performance..... 3-1
Table 3-2. Surface performance summary. 3-4

FIGURES

Figure 1-1. Daily maximum 8-hour ozone concentration time series for Texas metropolitan areas for June 1-July 2, 2006. Time series provided by Pete Breitenbach, TCEQ..... 1-1
Figure 1-2. Daily maximum 8-hour ozone concentrations for Texas metropolitan areas for June 1-July 2, 2006. Chart provided by Pete Breitenbach, TCEQ..... 1-3

Figure 2-1. MM5 Modeling Domain and NOAA NPN tropospheric profiler sites (blue triangles) 2-5
Figure 3-1. METSTAT evaluation subdomains 3-5
Figure 3-2. Wind speed and direction performance soccer plot 3-6
Figure 3-3. Wind speed performance soccer plot. 3-7
Figure 3-4. DFW area wind speed time series 3-8
Figure 3-5. San Antonio area wind speed time series. 3-8
Figure 3-6. Austin area wind speed time series 3-9
Figure 3-7. Tyler-Longview-Marshall area wind speed time series. 3-9
Figure 3-8. DFW wind direction time series 3-10
Figure 3-9. San Antonio wind direction time series. 3-10
Figure 3-10. Austin wind direction time series 3-11
Figure 3-11. Tyler-Longview-Marshall wind direction time series. 3-11
Figure 3-12. Temperature performance soccer plot 3-12
Figure 3-13. DFW area temperature time series. 3-13
Figure 3-14. San Antonio area temperature time series 3-14
Figure 3-15. Austin area temperature time series. 3-15
Figure 3-16. Tyler-Longview-Marshall area temperature time series. 3-16
Figure 3-17. Humidity performance soccer plot 3-17
Figure 3-18. DFW area humidity time series. 3-18
Figure 3-19. San Antonio area humidity time series 3-19
Figure 3-20. Austin area humidity time series 3-20
Figure 3-21. Tyler-Longview-Marshall area humidity time series 3-21
Figure 3-22. Wind performance soccer plot in which evaluation is performed using both CAMS and ds472 datasets 3-22
Figure 3-23. Top two panels: wind speed time series for DFW area ds472 (black) and CAMS (red) monitors and difference (blue). Bottom two panels: wind direction time series for DFW area ds472 (black) and CAMS (red) monitors and difference (blue). 3-23
Figure 4-1. Episode precipitation totals (mm). Top panel: CPC observed precipitation. Bottom panel: MM5 precipitation on the 12 km grid. 4-4
Figure 4-2. Episode precipitation totals (mm). Top left panel: CPC observed precipitation in the region spanned by the 4 km grid. Top right panel: MM5 precipitation on the 12 km grid in the 4 km grid region. Lower left panel: MM5 precipitation on the 4 km grid. 4-5
Figure 4-3. Daily precipitation totals (mm) for May 29-June 1, 2006. Left hand column: CPC observed precipitation in the region spanned by the 4 km grid. Center column: MM5 precipitation on the 12 km grid in the 4 km grid region. Right hand column: MM5 precipitation on the 4 km grid 4-6
Figure 4-4. Daily precipitation totals (mm) for June 6-8, 2006. Left hand column: CPC observed precipitation in the region spanned by the 4 km grid. Center column: MM5 precipitation on the 12 km grid in the 4 km grid region. Right hand column: MM5 precipitation on the 4 km grid. 4-8

Figure 4-5. Daily precipitation totals (mm) for June 13-16, 2006. Left hand column: CPC observed precipitation in the region spanned by the 4 km grid. Center column: MM5 precipitation on the 12 km grid in the 4 km grid region. Right hand column: MM5 precipitation on the 4 km grid. 4-9

Figure 4-6. Daily precipitation totals (mm) for June 17-20, 2006. Left hand column: CPC observed precipitation in the region spanned by the 4 km grid. Center column: MM5 precipitation on the 12 km grid in the 4 km grid region. Right hand column: MM5 precipitation on the 4 km grid. 4-10

Figure 4-7. Daily precipitation totals (mm) for June 21-24, 2006. Left hand column: CPC observed precipitation in the region spanned by the 4 km grid. Center column: MM5 precipitation on the 12 km grid in the 4 km grid region. Right hand column: MM5 precipitation on the 4 km grid. 4-11

Figure 4-8. Daily precipitation totals (mm) for June 25, 2006. Left hand column: CPC observed precipitation in the region spanned by the 4 km grid. Center column: MM5 precipitation on the 12 km grid in the 4 km grid region. Right hand column: MM5 precipitation on the 4 km grid. 4-12

Figure 4-9. Daily precipitation totals (mm) for June 28-July 1, 2006. Left hand column: CPC observed precipitation in the region spanned by the 4 km grid. Center column: MM5 precipitation on the 12 km grid in the 4 km grid region. Right hand column: MM5 precipitation on the 4 km grid. 4-13

Figure 5-1. June 18, DFW. Upper left hand panel: MM5 hourly total precipitation (mm) on the 12 km grid. Upper right hand panel: MM5 hourly total precipitation (mm) on the 4 km grid. Upper center panel: observed (black) and predicted (red) wind direction time series for the DFW area on the 12 km grid. Lower center panel: observed (black) and predicted (red) wind direction time series for the DFW area on the 4 km grid 5-6

Figure 5-2. DFW, June 18. Upper left hand panel: MM5 12 km grid precipitation for the hour 1800 CDT. Upper right hand panel: MM5 4 km grid precipitation for the hour 1800 CDT. Lower left hand panel: GOES-12 visible satellite image from 2315 Z (1815 CDT) on June 18 5-7

Figure 5-3. San Antonio, June 13. Upper left hand panel: MM5 12 km grid precipitation for the hour 1800 CDT. Upper right hand panel: MM5 4 km grid precipitation for the hour 1800 CDT. GOES-12 visible satellite image from 2315 Z (1815 CDT) on June 13 5-8

Figure 5-4. June 13-14, San Antonio. Upper panel: observed (black) and predicted (red) wind direction time series for the San Antonio area on the 12 km grid. Lower center panel: observed (black) and predicted (red) wind direction time series for the San Antonio area on the 4 km grid 5-9

Figure 5-5. June 14. Upper right hand panel: MM5 12 km grid precipitation for the hour 1800 CDT. Upper left hand panel: MM5 4 km grid precipitation for the hour 1800 CDT. Visible satellite image from 2315 Z (1815 CDT) on June 14..... 5-10

Figure 5-6. June 7, TLM. Upper left hand panel: MM5 hourly total precipitation (mm) on the 12 km grid. Upper right hand panel: MM5 hourly total precipitation (mm) on the 4 km grid. Upper center panel: observed (black) and predicted (red) wind direction time series for the TLM area on the 12 km grid. Lower center panel: observed (black) and predicted (red) wind direction time series for the TLM area on the 4 km grid..... 5-11

Figure 5-7. June 7, TLM. Upper right hand panel: MM5 12 km grid precipitation for the hour 1500 CDT. Upper left hand panel: MM5 4 km grid precipitation for the hour 1500 CDT. MODIS AQUA visible satellite image from 1951-2002 Z (1451-1502 CDT) on June 7. 5-12

Figure 5-8. June 12, TLM. Upper left hand panel: CPC observed daily precipitation total (mm). Upper right hand panel: MM5 daily precipitation total (mm) on the 12 km grid. Lower right hand panel: MM5 daily precipitation total (mm) on the 4 km grid. 5-13

Figure 5-9. June 12. Observed (black) and predicted (red) wind direction time series for the TLM area on the 12 km grid. Lower center panel: observed (black) and predicted (red) wind direction time series for the TLM area on the 4 km grid..... 5-14

Figure 5-10. June 12, TLM. Upper right hand panel: MM5 12 km grid precipitation for the hour 1800 CDT. Upper left hand panel: MM5 4 km grid precipitation for the hour 1800 CDT. GOES-12 visible satellite image from 2315 Z (1815 CDT) on June 12..... 5-15

EXECUTIVE SUMMARY

At the request of TCEQ, ENVIRON has conducted MM5 modeling of the period May 29-July 3, 2006. This period corresponds to extended episodes of high ozone in North and Central Texas as well as the Houston area. The MM5 modeling database described in this report may potentially be used in support of future ozone modeling focused on the San Antonio and Austin areas; therefore, the focus of this study was on evaluation of model performance over these areas, as well as the Dallas-Fort Worth and Tyler-Longview-Marshall regions.

Here follows a summary of MM5 performance in the initial modeling of the May 29-July 3, 2006 extended Texas ozone episode.

Comparison of Performance on 12 km versus 4 km Grids

- Model performance degraded for both wind speed and wind direction on the 4 km grid relative to the 12 km grid.
- Model performance improved for temperature and humidity on the 4 km grid relative to the 12 km grid.
- Precipitation on the 4 km grid tends to be confined to smaller areas and to have higher maxima, while precipitation tends to occur over a larger area on the 12 km grid, and to have lower maxima.
- Observed daily precipitation totals were not well simulated by the model on either the 12 km or the 4 km grid.
- The episode total precipitation pattern over Texas was reproduced with greater fidelity on the 4km grid than on the 12 km grid.

Surface Wind Performance

- On both the 4 km and 12 km grids, MM5 met the performance benchmark for wind speed for all four regions (Dallas-Fort Worth, San Antonio, Austin, and Tyler-Longview-Marshall).
- The wind direction performance met the benchmark on the 12 km grid for Dallas-Fort Worth, but not for San Antonio, Austin, or Tyler-Longview-Marshall.

Surface Humidity Performance

- Model performance was within the benchmark for humidity on the 4 km and 12 km grids for all four regions.
- On the 12 km grid, the model showed a wet bias, and this wet bias was reduced for all regions in going to the 4 km grid.
- The reduction in wet bias was due to better simulation of the daily minima in humidity in the 4 km run. On the 12 km grid, the model remained too wet during the minima.

Surface Temperature Performance

- Temperature performance showed a general cold bias.

- On the 12 km grid, only San Antonio was within the benchmark for temperature bias, and all four regions failed to meet the temperature error benchmark.
- On the 4 km grid, temperature performance improved so that all regions but TLM met the benchmark for bias. All four regions remained outside the benchmark for error on the 4 km grid.

Assessment of Anomalous Convection

- Anomalous convection was present during many days of the simulation, but occurred on only a small number of high ozone days. On a subset of these high ozone days, anomalous convection may have degraded the wind performance, but was unlikely to have been the only contributing factor.

This initial MM5 run can serve as a good starting point for the development of a meteorological database for future ozone modeling of the May 29-July 3, 2006 episode. The performance of the initial run was encouraging, but further work should be undertaken to improve the surface performance so that the model meets most performance benchmarks, to improve precipitation performance, and to reduce the incidence of anomalous convection on high ozone days. A primary goal is the improvement of the wind direction performance. A series of sensitivity tests is proposed to address the issues noted above and to optimize model performance over the San Antonio/Austin and Dallas/Tyler-Longview-Marshall areas.

1. INTRODUCTION

At the request of TCEQ, ENVIRON has conducted MM5 modeling of the period May 29-July 3, 2006. This period encompasses extended episodes of high ozone in North and Central Texas as well as the Houston area. Figure 1-1 shows time series of the daily maximum 8-hour ozone concentration for Texas metropolitan areas for June 1-July 2, 2006. Figure 1-2 displays this data in tabular form. The data show that the episode is comprised of a period of high ozone in Texas from June 2-June 15, followed by a period of cleaner air from June 16-23, except in the Dallas-Fort Worth area, which experiences high ozone on June 18. A second episode of high ozone occurs over much of Texas on June 27-July 1, with the onset of high ozone occurring earlier along the Gulf Coast.

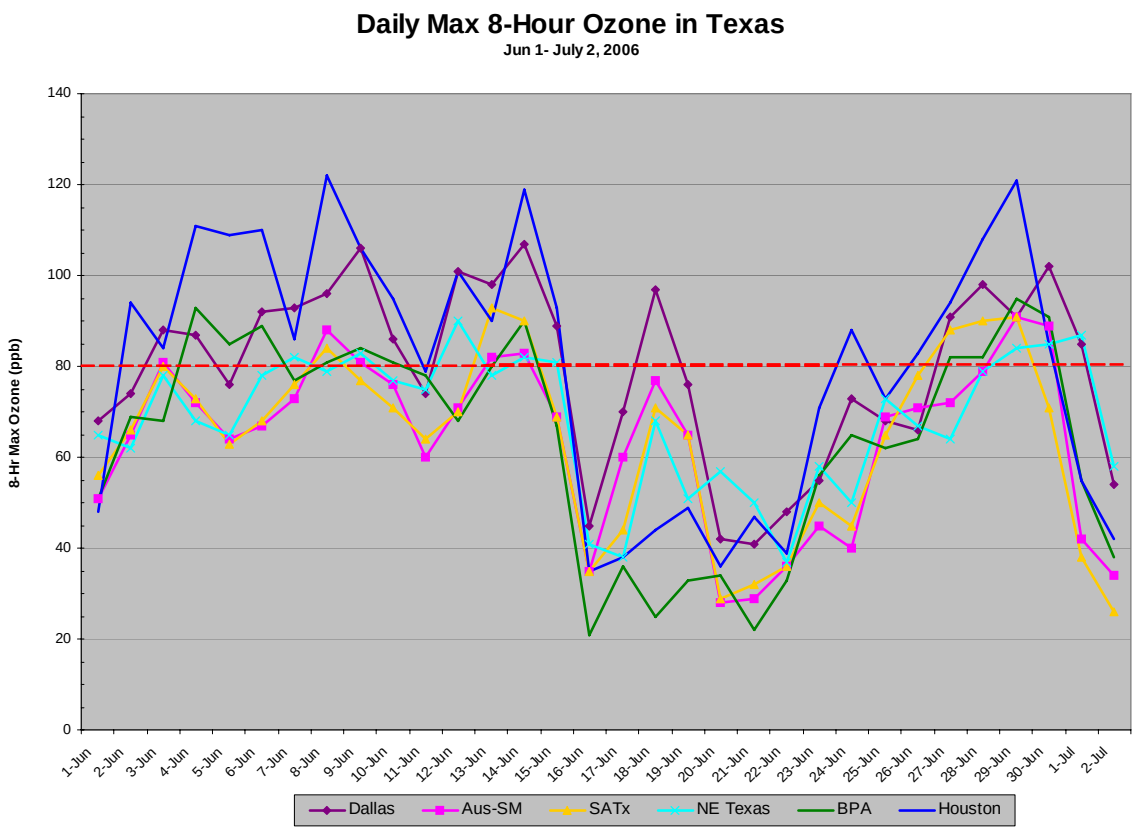

Figure 1-1. Daily maximum 8-hour ozone concentration time series for Texas metropolitan areas for June 1-July 2, 2006. Time series provided by Pete Breitenbach, TCEQ.

The MM5 modeling database described in this report may potentially be used in support of future ozone modeling focused on the San Antonio and Austin areas; therefore, the emphasis of this study was on evaluation of model performance over these areas, as well as the Dallas-Fort Worth and Tyler-Longview-Marshall regions. TCEQ has modeled a subset of this episode, May 29-June 17, and their simulation provided a starting point for the model configuration for the ENVIRON MM5 run.

In this report, we document the configuration of ENVIRON's initial 108/36/12/4 km nested MM5 simulation of May 29-July 3, 2006, and evaluate the model's performance over the San Antonio, Austin, Dallas-Fort Worth, and Tyler-Longview-Marshall areas on the 12 km and 4 km grids. We examine the model's surface performance and compare model-predicted precipitation to observed precipitation. Modeled precipitation fields and satellite imagery are examined to determine whether anomalous convection was present during the simulation; where anomalous convection was present during high ozone periods, the modeled wind fields are reviewed to assess whether the anomalous convection may have degraded the wind performance. Finally, we make recommendations for a series of sensitivity tests aimed at improving model performance in future simulations of this episode.

2006 Eight Hour Ozone Data

Area	Highest Daily Maximum by Area																	Estimated Local Add-On (High Minus Lowest Daily Max)												# Monitors with High Ozo				
City	Dallas-Fort Worth	Oklahoma South	Texas Northeast	Tyler	Longview-Marshall	Shreveport LA	Texas East Central	Beaumont-Port Arthur	Houston-Galveston-Brazoria	Austin	San Antonio	Texas Central East	Victoria	Corpus Christi	Laredo	McAllen-Edinburg-Mission	Brownsville-Harlingen	Dallas-Fort Worth	Tyler	Longview-Marshall	Beaumont-Port Arthur	Houston-Galveston-Brazoria	Austin	San Antonio	Victoria	Corpus Christi	Laredo	McAllen-Edinburg-Mission	Brownsville-Harlingen	El Paso	DFW Count if >80	TLM Count if >80	Austin Count if >80	SATx Count if >80	BPA Count if >80
05/30 Tue	52	57	45	33	40	53	28	45	35	47	58	38	31	36	31	37	32	16	2	9	21	11	14	25	2	7	8	14	9	23					
05/31 Wed	56	47	56	56	44	37	45	64	55	36	43	47	37	36	28	38	36	15	24	12	37	28	8	15	6	5	0	10	8	32					
06/01 Thu	68	63	65	59	65	58	54	51	48	51	56	53	36	36	29	33	30	**24**	14	**20**	19	16	18	**23**	7	7	2	6	3	**24**	0	0	0	0	0
06/02 Fri	74	73	62	59	62	59	55	69	94	65	66	45	43	34	26	30	32	16	13	16	**25**	**50**	**20**	**21**	10	1	0	4	6	**29**	0	0	0	0	0
06/03 Sat	88	73	78	78	75	71	67	68	84	81	80	64	62	55	31	27	25	**25**	**20**	17	18	**34**	**22**	**21**	7	0	10	6	4	**33**	6	0	1	0	0
06/04 Sun	87	78	68	68	67	88	64	93	111	72	73	54	44	30	33	29	25	**23**	5	4	**51**	**69**	**20**	**21**	14	0	10	6	2	**26**	3	0	0	0	4
06/05 Mon	76	81	65	58	65	66	63	85	109	64	63	61	62	38	31	30	35	**22**	4	11	**29**	**53**	16	15	**24**	0	11	10	15	**23**	0	0	0	0	4
06/06 Tue	92	71	78	74	59	71	65	89	110	67	68	65	66	45	30	30	54	**30**	**28**	13	**32**	**53**	15	16	**21**	0	4	4	**28**	**20**	4	0	0	0	5
06/07 Wed	93	68	82	82	79	65	54	77	86	73	76	64	61	52	41	56	55	**28**	**34**	**31**	**26**	**35**	**30**	**33**	9	0	0	15	14	13	3	1	0	0	0
06/08 Thu	96	75	79	79	68	61	65	81	122	88	84	65	61	52	45	53	46	**37**	**21**	10	**28**	**69**	**25**	**21**	9	0	1	9	2	14	5	0	1	1	1
06/09 Fri	106	97	83	73	83	84	66	84	106	81	77	70	65	52	44	54	51	**36**	7	17	**24**	**46**	**24**	**20**	14	1	0	10	7	17	10	1	1	0	3
06/10 Sat	86	78	77	75	77	79	70	81	95	76	71	69	63	52	45	49	51	18	6	8	**24**	**38**	16	11	12	1	1	5	7	17	2	0	0	0	2
06/11 Sun	74	74	75	59	70	76	67	78	79	60	64	55	55	51	41	37	32	**20**	5	16	**31**	**32**	18	**22**	**21**	17	9	5	0	11	0	0	0	0	0
06/12 Mon	101	68	90	80	90	73	69	68	101	71	70	52	45	32	30	31	19	**39**	17	**27**	**24**	**57**	**28**	**27**	17	4	11	12	0	12	7	2	0	0	0
06/13 Tue	98	69	78	73	63	67	63	80	90	82	93	74	60	47	39	45	29	**42**	**20**	10	**44**	**54**	**24**	**35**	18	5	18	**24**	8	**23**	11	0	1	3	0
06/14 Wed	107	81	82	82	79	72	67	90	119	83	90	81	64	69	43	49	61	**37**	14	11	**26**	**55**	12	19	**20**	**25**	0	6	18	10	7	1	3	6	5
06/15 Thu	89	98	81	77	75	79	71	67	93	69	69	65	69	67	42	50	62	19	10	8	14	40	16	16	12	10	0	8	**20**	13	10	2	0	0	0
06/16 Fri	45	55	41	39	29	38	31	21	35	35	35	30	21	22	22	19	18	13	15	5	6	**20**	15	15	5	6	6	3	2	**22**	0	0	0	0	0
06/17 Sat	70	68	38	38	36	33	39	36	38	60	44	44	24	19	23	22	19	**21**	14	12	**21**	**23**	**25**	9	6	1	6	5	2	**20**	0	0	0	0	0
06/18 Sun	97	83	68	41	34	32	41	25	44	77	71	64	36	25	20	17	15	**39**	14	7	11	**30**	**26**	**20**	16	5	7	4	2	**27**	9	0	0	0	0
06/19 Mon	76	80	51	36	44	45	28	33	49	65	65	55	32	18	35	17	14	**34**	5	13	10	**26**	17	17	16	2	**22**	4	1	17	0	0	0	0	0
06/20 Tue	42	55	57	32	37	43	36	34	36	28	29	27	31	19	26	18	17	11	6	11	14	16	7	8	15	3	11	3	2	**26**	0	0	0	0	0
06/21 Wed	41	44	50	35	34	46	30	22	47	29	32	28	19	21	26	20	22	16	6	5	10	**35**	7	10	1	3	8	2	4	**24**	0	0	0	0	0
06/22 Thu	48	40	37	33	35	39	31	33	39	36	36	32	27	20	24	19	18	**20**	10	12	15	**21**	13	13	9	2	7	2	1	19	0	0	0	0	0
06/23 Fri	55	60	58	43	58	54	39	56	71	45	50	42	30	22	26	21	19	**23**	15	**30**	**36**	**51**	16	**21**	10	2	11	6	4	17	0	0	0	0	0
06/24 Sat	73	62	50	45	50	46	45	65	88	40	45	45	31	25	29	25	23	**24**	0	5	**37**	**60**	9	14	9	3	8	4	2	16	0	0	0	0	0
06/25 Sun	68	64	73	69	73	60	54	62	73	69	65	64	61	58	34	33	31	8	16	**20**	**22**	**33**	19	15	18	15	12	11	9	16	0	0	0	0	0
06/26 Mon	66	54	67	63	67	50	67	64	83	71	78	70	90	68	65	55	50	15	10	14	14	**33**	12	19	**28**	6	**23**	13	8	18	0	0	0	0	0
06/27 Tue	91	61	64	64	62	64	62	82	94	72	88	70	76	82	54	65	62	**33**	14	12	**26**	**38**	11	**27**	**25**	**31**	0	11	8	16	6	0	0	3	1
06/28 Wed	98	86	79	76	79	68	55	82	108	79	90	80	76	78	60	63	61	**28**	13	16	**24**	**50**	15	**26**	4	6	2	5	3	16	8	0	0	8	2
06/29 Thu	91	91	84	77	84	89	72	95	121	91	91	78	70	66	52	43	43	**29**	10	17	**27**	**53**	19	19	9	5	**21**	12	12	**20**	5	1	4	9	5
06/30 Fri	102	97	85	81	84	83	74	91	85	89	71	69	50	26	27	23	23	**31**	8	11	**37**	**31**	**43**	**25**	**29**	5	7	3	3	**24**	7	4	4	0	3
07/01 Sat	85	83	87	51	80	83	55	55	55	42	38	39	28	27	21	22	24	**37**	3	**32**	**21**	**21**	17	13	5	4	1	2	4	15	2	1	0	0	0
07/02 Sun	54	51	58	46	52	60	36	38	42	34	26	37	30	29	26	26	27	**25**	9	15	15	19	13	5	4	3	5	5	6	15	0	0	0	0	0

Figure1-2. Daily maximum 8-hour ozone concentrations for Texas metropolitan areas for June 1-July 2, 2006. Chart provided by Pete Breitenbach, TCEQ.

2. MM5 CONFIGURATION

In this section, we describe the MM5 configuration used in the simulation, noting differences from the TCEQ modeling of the May 29-June 17, 2006 period. ENVIRON has adopted the horizontal and vertical grid structure used by TCEQ for its modeling of 2005 and 2006, including a nested 4 km grid that encompasses the Dallas/TLM and San Antonio/Austin areas. Figure 1 shows the MM5 nested domain configuration. The grids have resolutions of 108 km, 36 km, 12 km, and 4 km, and the number of rows and columns for each grid is 53x43, 97x76, 145x100, 184x166, respectively. The three coarse domains were run with two-way nesting using 1 point feedback with light smoothing, while the 4 km domain was run with one-way nesting using the 12 km MM5 model output to generate the 4 km domain input through the MM5 NESTDOWN processor.

The vertical structure used is shown in Table 2-1. Reference state parameters used to derive the pressures, altitudes, and layer thicknesses corresponding to the sigma levels are: P0=1013 mb, TS0=304.00 K, reference temperature lapse rate=45 K, and PTOP=50 mb. The model has 43 vertical layers extending from the surface up to approximately 20 km. The surface layer is roughly 34 meters thick.

Table 2-1. MM5 vertical layer structure.

Layer	Sigma	Pressure (mb)	Height (m)	Thickness (m)
43	0.0000	50.00	20820.97	890.18
42	0.0100	59.63	19930.79	1152.48
41	0.0250	74.08	18778.31	1296.15
40	0.0450	93.34	17482.16	1103.86
39	0.0650	112.60	16378.30	1188.86
38	0.0900	136.67	15189.44	1033.53
37	0.1150	160.75	14155.91	1088.51
36	0.1450	189.64	13067.40	962.55
35	0.1750	218.53	12104.85	1000.66
34	0.2100	252.23	11104.19	1018.20
33	0.2500	290.75	10085.99	913.19
32	0.2900	329.27	9172.80	829.18
31	0.3300	367.79	8343.63	760.31
30	0.3700	406.31	7583.32	617.73
29	0.4050	440.02	6965.59	579.58
28	0.4400	473.72	6386.01	546.18
27	0.4750	507.43	5839.83	516.68
26	0.5100	541.13	5323.14	421.86
25	0.5400	570.02	4901.29	404.30
24	0.5700	598.91	4496.98	388.25
23	0.6000	627.80	4108.73	373.51
22	0.6300	656.69	3735.22	359.92
21	0.6600	685.58	3375.30	347.36
20	0.6900	714.47	3027.94	335.70
19	0.7200	743.36	2692.24	324.85
18	0.7500	772.25	2367.39	262.95
17	0.7750	796.33	2104.43	256.31
16	0.8000	820.40	1848.13	250.01
15	0.8250	844.48	1598.12	244.04
14	0.8500	868.55	1354.08	143.68
13	0.8650	883.00	1210.39	141.70
12	0.8800	897.44	1068.69	139.78
11	0.8950	911.89	928.92	137.91
10	0.9100	926.33	791.01	90.93
9	0.9200	935.96	700.08	90.13
8	0.9300	945.59	609.95	89.36
7	0.9400	955.22	520.59	88.59
6	0.9500	964.85	432.00	87.84
5	0.9600	974.48	344.15	87.11
4	0.9700	984.11	257.04	86.39
3	0.9800	993.74	170.66	85.68
2	0.9900	1003.37	84.98	51.07
1	0.9960	1009.15	33.91	33.91
0	1.0000	1013.00	0.00	

MM5 Physics Options

ENVIRON retained most of the physics options selected in TCEQ's initial MM5 run. One difference is the use of the Grell cumulus parameterization on the 108 km domain rather than using no parameterization of cumulus convection, as was done in the TCEQ run. At a grid resolution of 108 km, updraft and downdraft circulations due to cumulus convection cannot be resolved by the model and should be parameterized (Molinari, 1993). The Grell parameterization is appropriate for use at 108 km resolution (PSU/NCAR, 2005), and was chosen in order to be consistent with the cumulus parameterizations used on the 36 km and 12 km domains.

A second departure from the TCEQ configuration is that the shallow convection option is turned off in the ENVIRON simulation. The shallow convection scheme treats shallow, non-precipitating clouds that are driven by PBL destabilization. These clouds are assumed to have small radii, strong entrainment, and no downdrafts. The parameterization is based on the Arakawa-Schubert and Grell cumulus schemes, and posits an equilibrium between the cloud activity and the PBL forcing. The guidance from the developers of MM5 is that this scheme has a small effect on model performance that does not justify the computational cost of its use (PSU/NCAR, 2005). The TCEQ and ENVIRON column physics options are summarized in Table 2-2 below.

Table 2-2. Physics options in the TCEQ and ENVIRON MM5 simulations.

	TCEQ		ENVIRON	
	108/36/12 km	**4 km**	**108/36/12 km**	**4 km**
Cumulus Parameterization	None/Grell/Grell	None	Grell/Grell/Grell	None
Shallow convection	Yes	Yes	No	No
Radiation (LW/SW)	RRTM/Dudhia	RRTM/Dudhia	RRTM/Dudhia	RRTM/Dudhia
Cloud Microphysics	Simple Ice	Simple Ice	Simple Ice	Simple Ice
PBL/LSM	ETA/NOAH LSM	ETA/NOAH LSM	ETA/NOAH LSM	ETA/NOAH LSM

Four Dimensional Data Assimilation (FDDA) Configuration

FDDA is used to nudge model predictions toward observational analyses and/or discrete measurements to control model "drift" from conditions that actually occurred. This approach has consistently been shown to provide powerful advantages in running mesoscale models for multi-day episodes, and has become the standard for photochemical applications. MM5 may be nudged toward gridded analyses ("analysis nudging") or toward individual observations ("observation nudging"). When analysis nudging is performed using three-dimensional gridded fields from a data set such as the Eta Data Assimilation System (EDAS), the technique is referred to as 3D analysis nudging. Analysis nudging may also be performed using gridded surface data; this is known as surface analysis nudging.

ENVIRON has enhanced MM5's observation nudging FDDA capabilities by developing software to incorporate wind observations of the troposphere from the NOAA Profiler Network

(NPN) into MM5 observation nudging files. This software was based on similar codes developed by TCEQ for integrating boundary layer profiler data into MM5 nudging files. For this extended episode, then, observation nudging was performed using winds from tropospheric profilers from the NPN as well as hourly surface winds from TDL US and Canada Hourly Surface Observations (ds472) archived at UCAR. TCEQ is currently preparing a data set of boundary layer profiler data from the TEXAQS II observing campaign. Although this data was not available at the time of the runs described in this report, it should be used in the sensitivity tests and model refinement proposed in Section 6. In addition, the EDAS analysis has been improved by including the ADP surface and upper air observations through the use of the LITTLE_R preprocessing program.

The configuration and nudging coefficients for observation nudging are shown in Table 2-3. Only observation nudging of surface winds is performed; temperature and humidity are not nudged. The ds472 data set was used for surface observation nudging of wind on the 108 km and 36 km domains, while the NOAA profiler data was used for observation nudging of wind on the 12 km and 4 km domains. Note that the Palestine, TX station is the only NOAA profiler station that lies within Texas on the 4 km grid (Figure 2-1). Surface and 3D grid analysis nudging were performed, and the nudging coefficients are displayed in Table 2-4. During the analysis of the run, it was noted that the nudging coefficient for 3D analysis nudging on the 12 km grid had inadvertently been set to zero. This will be corrected during the sensitivity tests recommended in Section 6.

Table 2-3. Coefficients for observation nudging.

	Nudging Coefficients (s^{-1})			
Nudged Field	**108 km**	**36 km**	**12 km**	**4km**
Winds	4.0×10^{-4}	4.0×10^{-4}	4.0×10^{-4}	4.0×10^{-4}
Temperature	n/a	n/a	n/a	n/a
Humidity	n/a	n/a	n/a	n/a

Table 2-4. Coefficients for grid analysis nudging.

	3D Nudging Coefficients (s^{-1})			
Nudged Field	**108 km**	**36 km**	**12 km**	**4km**
Winds	2.5×10^{-4}	1.0×10^{-4}	1.0×10^{-4}	n/a
Temperature	2.5×10^{-4}	1.0×10^{-4}	0	n/a
Humidity	1.0×10^{-5}	1.0×10^{-5}	1.0×10^{-5}	n/a
	Surface Nudging Coefficients (s^{-1})			
Winds	2.5×10^{-4}	1.0×10^{-4}	1.0×10^{-4}	n/a
Temperature	2.5×10^{-4}	1.0×10^{-4}	n/a	n/a
Humidity	1.0×10^{-5}	1.0×10^{-5}	n/a	n/a

Segmented MM5 Simulation Approach

The ozone episode under study covers the period May 29-July 3, 2006, and requires a 36-day simulation. The MM5 solution is subject to increasing error over the course of an extended

simulation due to uncertainties in initial/boundary conditions, limits in spatial and temporal resolution, and simplification and discretization in the governing equations. To reduce error propagation through the simulation, the model run was made in sequential 5-day run segments, and MM5 was re-initialized at the beginning of each 5-day period. Each 5-day segment had an initial spinup period of 24 hours that overlapped the last 24 hours of the preceding run. This segmented approach was successfully used in annual RPO MM5 simulations for WRAP, CENRAP, and VISTAS, and was shown to produce meteorological databases suitable for air quality modeling over extended time periods (Kemball-Cook *et al.* 2004). The May 29-July 3, 2006 episode simulation consisted of nine 5-day segments; each 5-day segment starts at 12 UTC and is 7200 minutes in length. The preliminary TCEQ simulation was performed in one temporal segment, with no restarts.

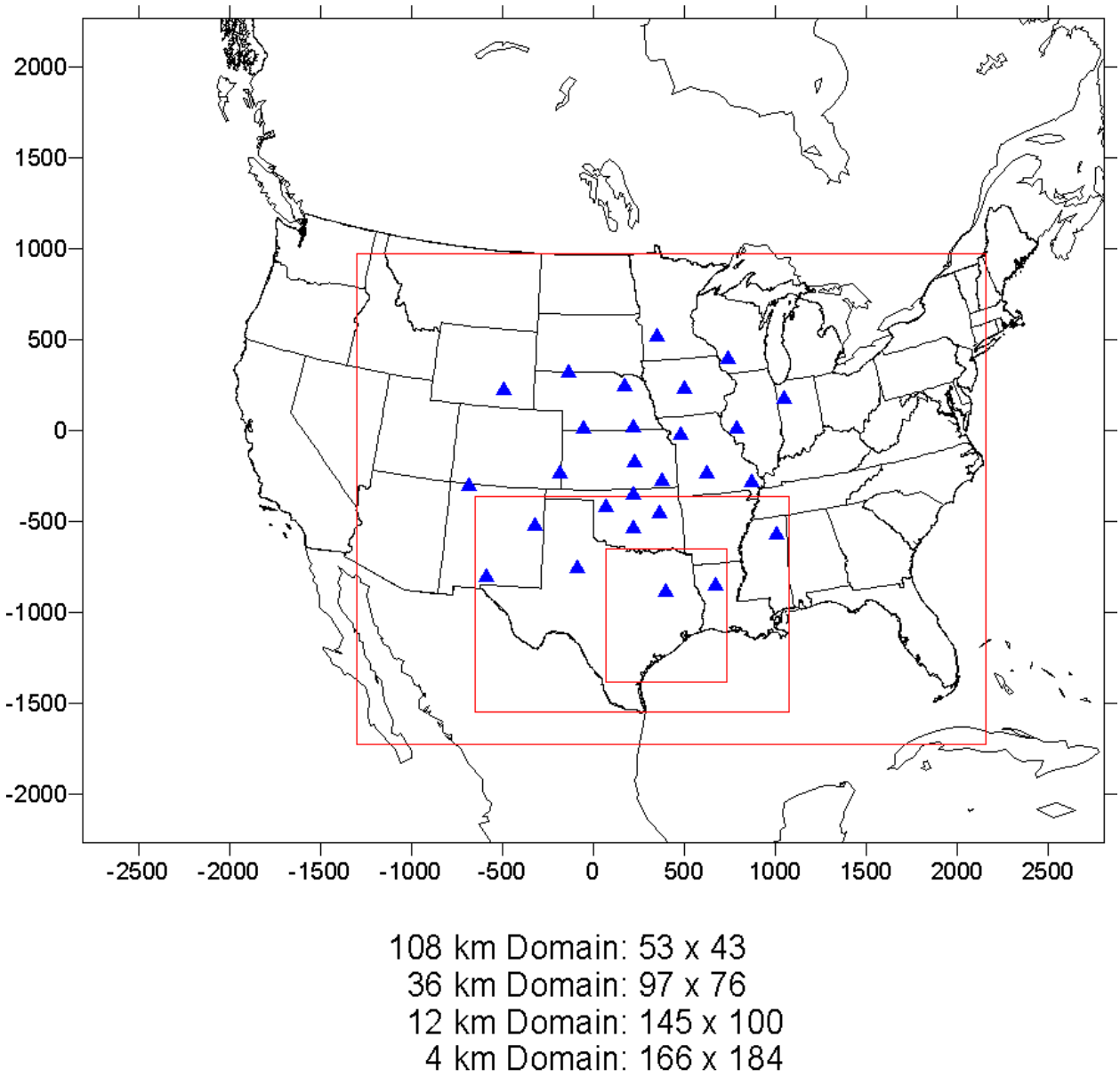

Figure 2-1. MM5 Modeling Domain and NOAA NPN tropospheric profiler sites (blue triangles).

3. MODEL EVALUATION APPROACH

METSTAT Surface Statistical Analysis

Emery *et al.* (2001) have derived a set of daily performance benchmarks for typical meteorological model performance. These standards were based upon the evaluation of approximately 30 MM5 and RAMS meteorological simulations executed in support of air quality applications, as reported by Tesche *et al*. (2001). The purpose of these benchmarks was not necessarily to give a passing or failing grade to any one particular meteorological model application, but rather to put its results into context and to allow the identification of potential problems in the MM5 fields. For example, expectations for meteorological model performance for a domain located in Alaska might be different for a Midwestern domain with simpler topography. The statistical performance benchmarks are given in Table 3-1.

Table 3-1. Statistical benchmarks for evaluating meteorological model performance.

	Wind Speed	Wind Direction	Temperature	Humidity
RMSE	≤ 2 m/s			
Mean Bias	≤ ±0.5 m/s	≤ ±10°	≤ ±0.5 K	≤ ±1 g/kg
Gross Error		≤ 30°	≤ 2 K	≤ 2 g/kg

The statistical evaluation of MM5 surface temperature and wind fields was performed using observations from TCEQ's Continuous Ambient Monitoring Station (CAMS) data set. Humidity data from CAMS was used in the Dallas-Fort Worth region, but for the other Texas regions the humidity evaluation was performed using NCAR dataset ds472, which contains hourly observations of the commonly measured variables from airports in the U.S. and Canada. This ensured that sufficient humidity data were available for METSTAT. The data of interest from CAMS and ds472 were extracted for the regions of interest and processed into the appropriate format for use in METSTAT.

MM5 performance during the May 29-July 3 episode was evaluated over the Dallas-Fort Worth (DFW), Austin (AUS), San Antonio (SA), and Tyler-Longview-Marshall (TLM) regions. CAMS monitors are each designated by TCEQ as belonging to a specific region of Texas, and these assignments were used in this analysis. The assignments may be found at: http://www.tceq.state.tx.us/compliance/monitoring/air/monops/sites/monitors_map.html, and are summarized in Figure 3-1. For each region, METSTAT was used to calculate hourly and daily statistical measures averaged across the region, and these were compared against benchmarks for acceptable model performance set forth by Emery *et al.* (2001) as summarized in Table 3-1.

In order to summarize the MM5's performance, we will show soccer plots on which are displayed average performance statistics for each region over the entire episode. Soccer plots are shown for wind speed RMSE versus wind direction error, wind speed bias versus wind speed RMSE, temperature bias versus temperature error, and humidity bias versus humidity error. In each plot, a solid blue line indicates the benchmark. A data point that falls inside the box represents a model run that meets the performance benchmark. Perfect model performance is indicated by a data point at (0,0). The closer a data point is to the origin, the better the model's performance.

Wind Performance

Soccer plots summarizing the wind speed and direction performance for the entire episode are shown in Figures 3-2 and 3-3. In all soccer plots, squares indicate the episode average for each region on the 12 km grid, while the triangles show the corresponding averages on the 4 km grid. The model run was within the performance benchmark for wind speed bias and RMSE for all four regions on the 12 km grid. On the 4 km grid, all regions were within the benchmark for RMSE, and only TLM was outside the benchmark for bias, with wind speeds that were too high, on average. Comparison of the 4 km and 12 km time series for TLM (Figure 3-7) confirms that winds speeds on the 4 km grid are generally higher and have a more pronounced tendency to overshoot the peaks during periods of higher observed winds than is seen on the 12 km grid. The hourly wind speed time series (Figures 3-4 through 3-7) reflect reasonably good performance with MM5 reproducing much of the observed variability. One period where the model has difficulty throughout the domain was the June 16-18 period, with wind speed peaks underestimated in DFW and San Antonio, and Austin (4 km grid only), and overestimated in TLM.

Performance for wind direction, however, was outside the benchmark on the 12 km grid for all regions but DFW. Performance degrades for both wind speed and wind direction in going from the 12 km grid to the 4 km grid. The wind direction time series for all regions show times of rapid changes in observed wind direction (for example, during the May 29-June 4 time period). MM5 often has difficulty reproducing these swings in the wind direction, (e.g. San Antonio, 4 km grid, on May 30, Figure 3-9) or mistiming them. When the observed wind direction variability lessens, model performance generally improves. By June 5, in the series of rapid wind shifts ends in Dallas and San Antonio (Figures 3-8 and 3-9), and the modeled wind direction time series more closely matches the observations.

Temperature Performance

Figure 3-12 is the soccer plot summarizing the temperature performance over the entire episode on both the 12 km and 4 km grids. There is a general cold bias on both grids. On the 12 km grid, all regions except San Antonio are outside the benchmark for bias, and all regions lie outside the error benchmark. Temperature bias performance shows a marked improvement for DFW, San Antonio, and Austin in going to the 4 km grid. These three regions lie within the bias benchmark on the 4 km grid. For the TLM area, performance deteriorates slightly for bias in going to the 4 km grid. For temperature error, performance improves very slightly for all regions but TLM, which shows a very small increase in error.

The time series show that for DFW (Figure 3-13), the model over predicted the amplitude of the diurnal cycle, with pronounced overestimation of the daily temperature maxima during the last week of the run. The model had difficulty reproducing the observed time series on June 3-4 and June 17-19 on the 12 km grid, and underestimated the daily maximum on all of these days. On the 4 km grid, the underestimate is either significantly reduced or replaced with a small overestimate on all of these days. Performance in San Antonio is similar, with the model showing a tendency to exaggerate the amplitude of the diurnal temperature cycle (Figure 3-14). As in DFW, there are a number of days when the model underestimates the daily temperature peak (June 3-4, June 16-18, and June 22-23) on the 12 km grid. The 4 km grid time series shows

that running with higher resolution improves the estimate of the peak on June 3-4 and June 16-17, but does not significantly improve on June 19 and turns the underestimate on the 12 km grid into an overestimate on June 22-23. For Austin, the model underestimates the observed peaks on the 12 km grid on May 30, June 2-3 and June 15-18. As with DFW and San Antonio, the underestimation of the daily peak is reduced or turned into a slight overestimate on the 4 km grid. For TLM, there is also a reduction of the cold bias in the simulation of the daily peaks, but the improvement is less dramatic than in the other regions

Temperature performance generally improves in going to the 4 km grid, and much of this can be attributed to the improved simulation of the daily temperature maxima during the periods June 2-4, June 16-18, and June 22-23. These are all times when rain is or has recently been present in the domain, and also show improvement in the humidity performance in going from the 12 km grid to the 4 km grid (Figures 3-18 through 3-22).

Humidity Performance

The humidity performance soccer plot is shown in Figure 3-17. The solid squares and triangles indicate that MM5 was evaluated using data from CAMS (DFW area only). The open squares and triangles indicate that performance was evaluated with respect to ds472 observations. There is an overall positive (wet) bias for all regions for this episode, with all regions lying within the performance benchmark on both the 4 km and 12 km grids. The soccer plot shows that the wet bias is reduced for all regions in going to the 4 km grid. The humidity time series (Figures 3-18 through 3-22) show that the reason for the reduction in wet bias is better simulation of the daily minima in humidity on the 4 km grid. The 12 km run tends to have smaller humidity variability than the observations, generally remaining too wet, while the 4 km grid simulation shows better agreement with observations simply by virtue of its lower minima. The periods June 8-14 in DFW and June 18-23 in San Antonio are examples of this. As noted above, the improved simulation of the humidity minima coincided with improved simulation of temperature maxima for June 2-4, June 16-18, and June 22-23 in DFW and SA.

Sensitivity of Results to Use of ds472 and CAMS Datasets for Evaluation

We examined the effect of using ds472 winds for the surface evaluation instead of winds from CAMS. Figure 3-22 shows the wind performance soccer plot with the evaluation performed using CAMS (solid squares for the 12 km grid, solid triangles for the 4 km grid) as well as ds472 (open squares for the 12 km grid, open triangles for the 4 km grid). The choice of dataset for the evaluation has a significant effect on the performance statistics, with the model faring worse when compared against ds472. Figure 3-23 compares wind speed and direction time series for the CAMS and ds472 dataset averages for the DFW area. ds472 has consistently higher wind speeds, with differences between the two data sets reaching values as high as 2 m/s. Wind direction time series also show significant differences. Further investigation into the differences between these data sets is warranted.

Surface Evaluation Summary

The model surface performance is summarized in Table 3-2. Entries in the table indicate whether the performance benchmark was met for a particular variable (temperature, etc.) on the 12 km and 4 km grids.

Table 3-2. Surface Performance Summary.

	Bias		Error		RMSE	
	12 km Grid	4 km Grid	12 km Grid	4 km Grid	12 km Grid	4 km Grid
Wind Speed	Yes	Yes, except TLM			Yes	Yes
Wind Direction			No, except DFW	No		
Temperature	Yes, except AUS	Yes, except TLM	No	No		
Humidity Bias	Yes	Yes	Yes	Yes		

- The episode average model performance is generally within the benchmarks for humidity, wind speed, and temperature bias.
- Episode average wind direction and temperature error did not meet the benchmarks.
- Addition of the 4 km grid improved performance for temperature and humidity, and degraded the wind performance.
- There is a general cold bias. In the 12 km run, all regions except SA are outside the benchmark for bias, and all are outside the benchmark for error.
- On the 4 km domain, temperature performance improved somewhat, so that all regions but TLM met the benchmark for bias. All four regions were still outside the benchmark for error.
- The humidity soccer plot shows that on the 12 km grid, the model has a wet bias, and its wet bias is reduced for all regions in going to the 4 km grid.
- The reason for the reduction in wet bias is better simulation of the daily minima in humidity in the 4 km runs. The 12 km run stays too humid.

MM5 4 km Domain and METSTAT Subdomains

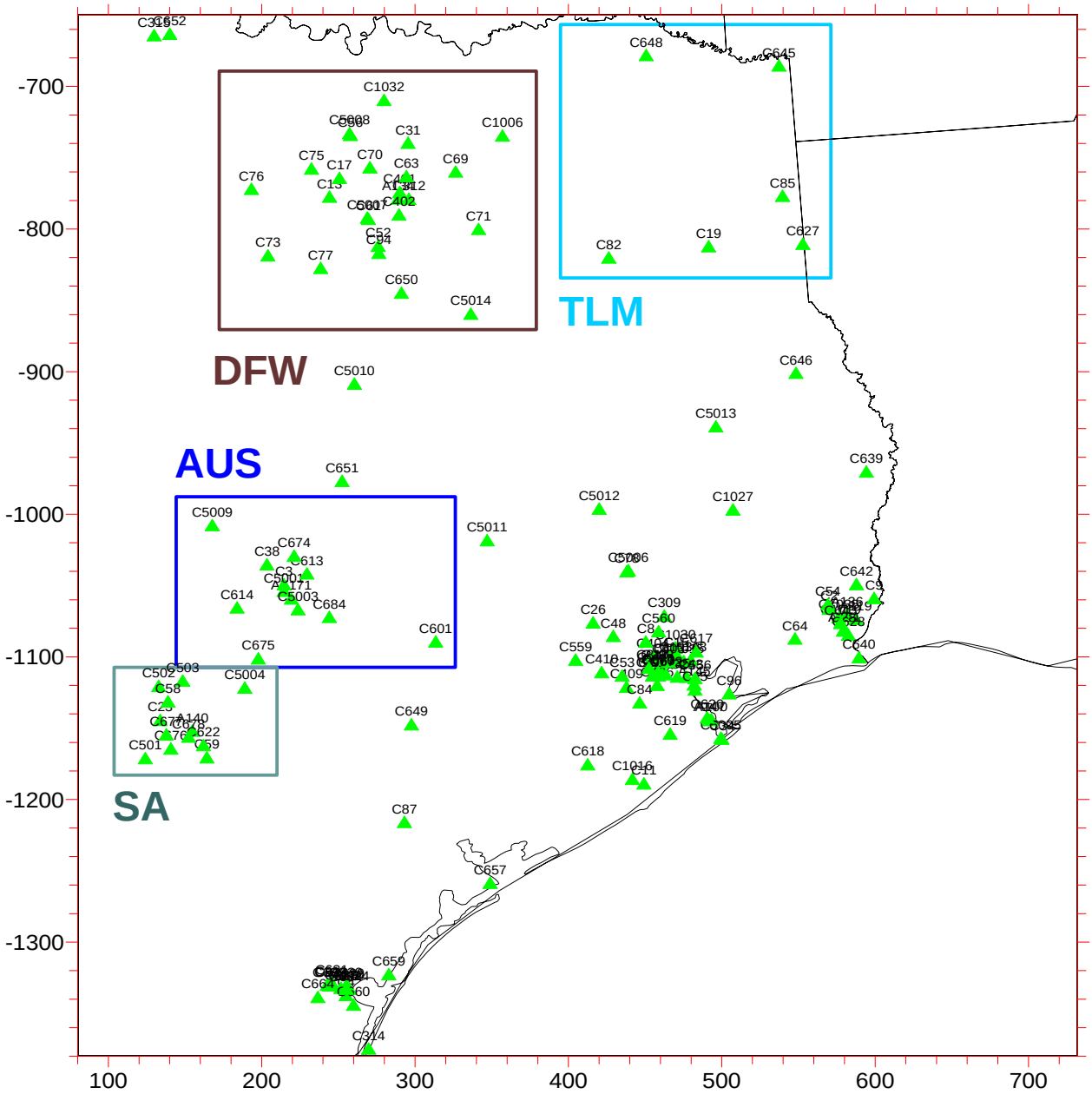

Figure 3-1. METSTAT evaluation subdomains.

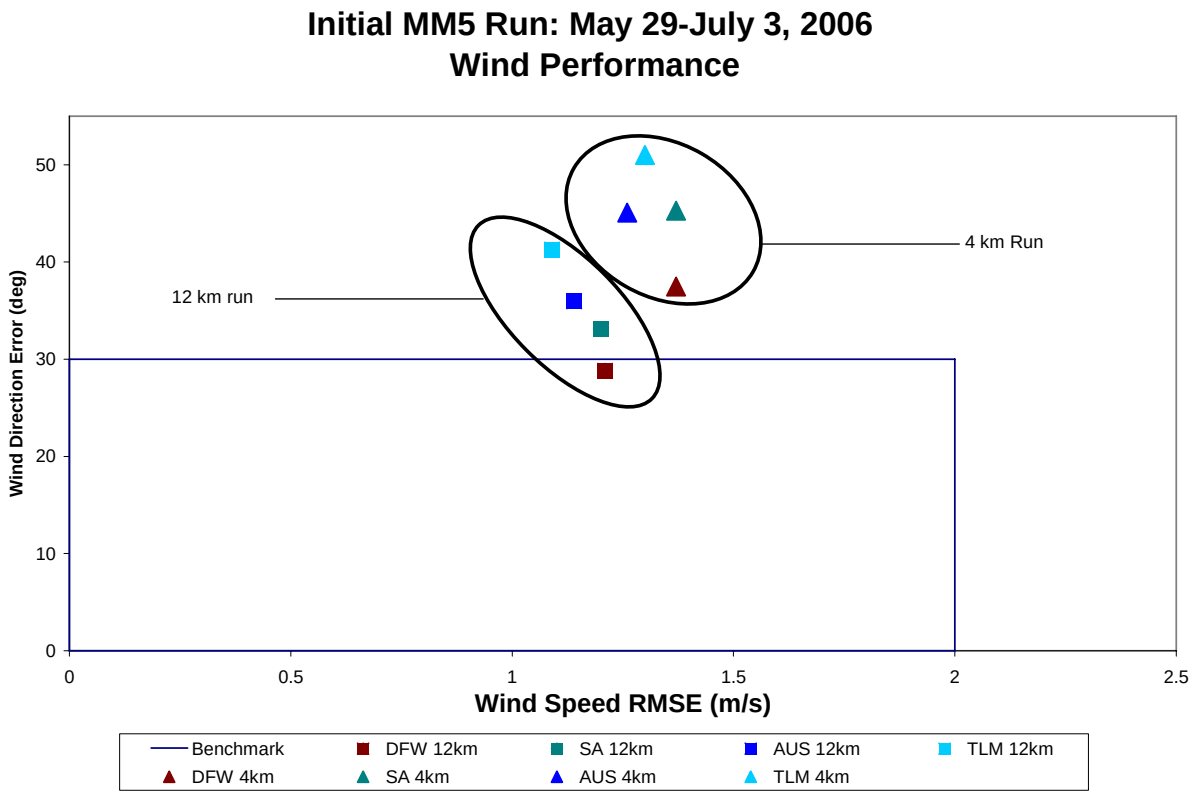

Figure 3-2. Wind speed and direction performance soccer plot.

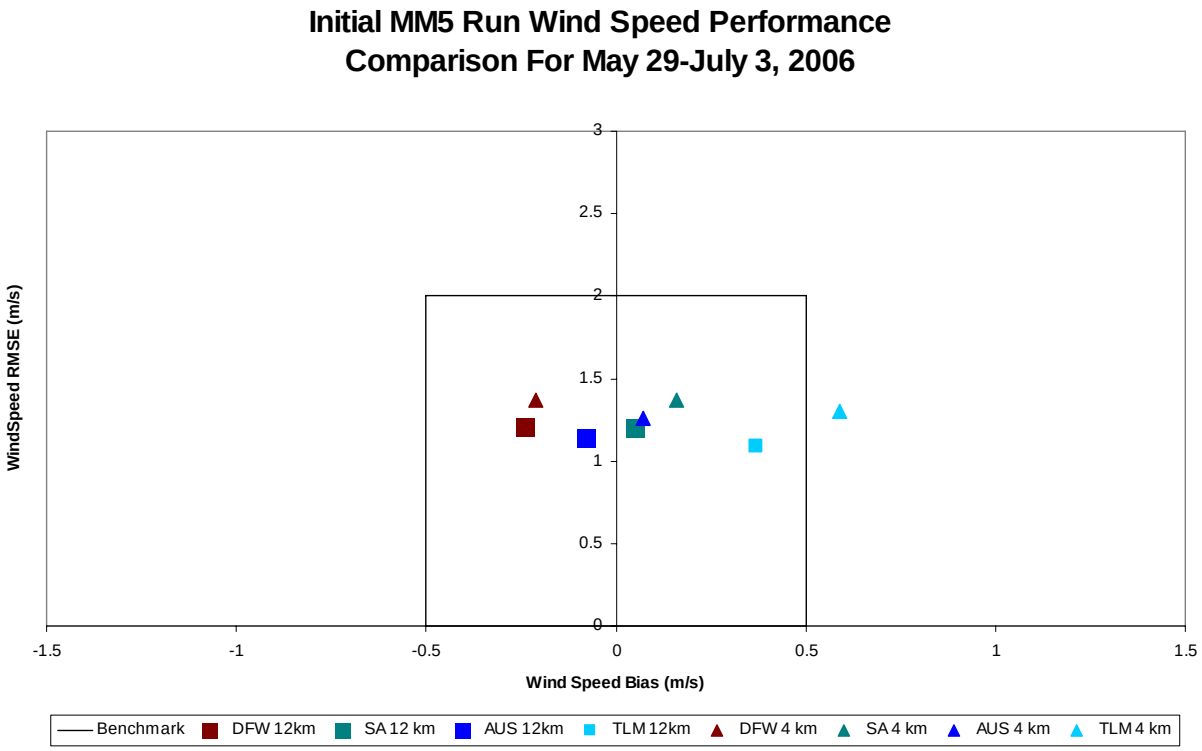

Figure 3-3. Wind speed bias and RMSE performance soccer plot.

DFW 12 km

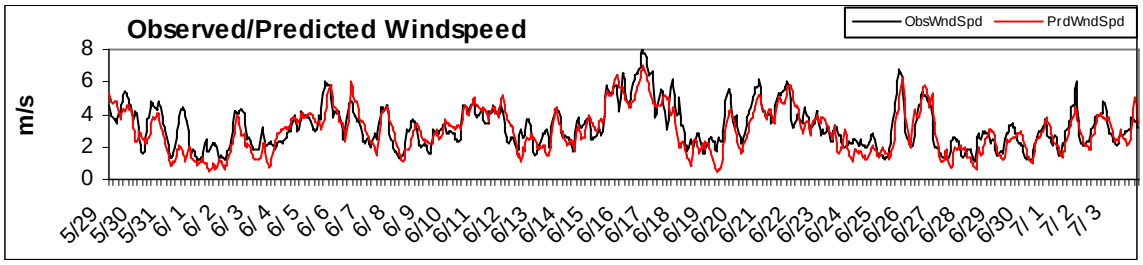

DFW 4 km

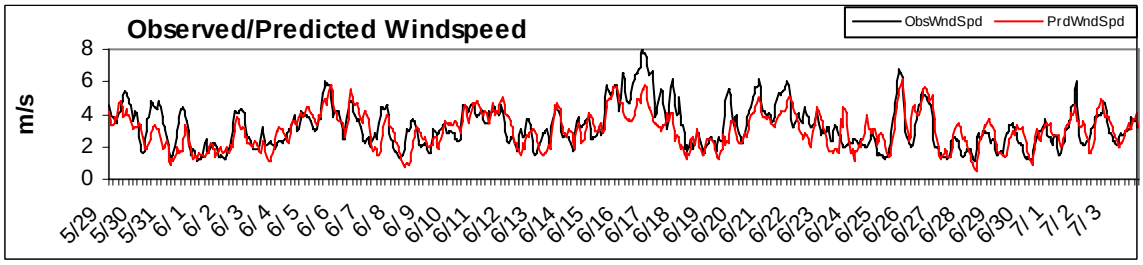

Figure 3-4. DFW area wind speed time series.

SA 12 km

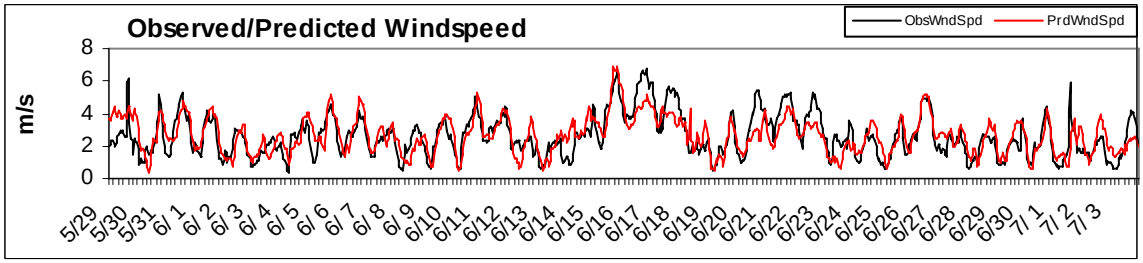

SA 4 km

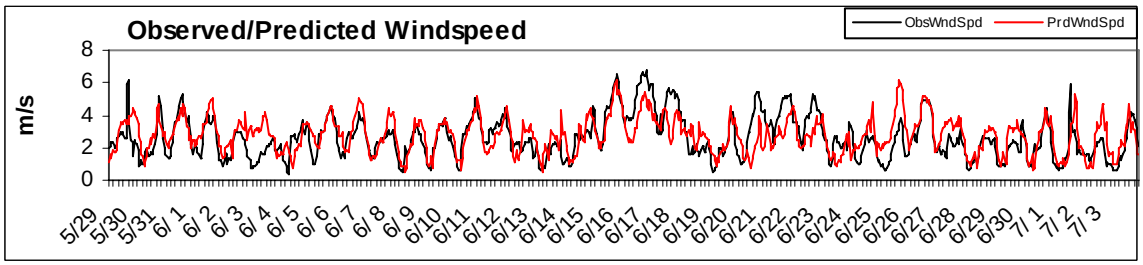

Figure 3-5. San Antonio area wind speed time series.

AUS 12 km

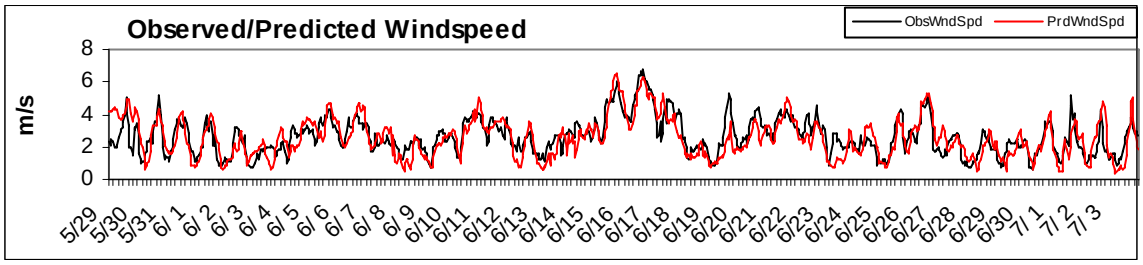

AUS 4 km

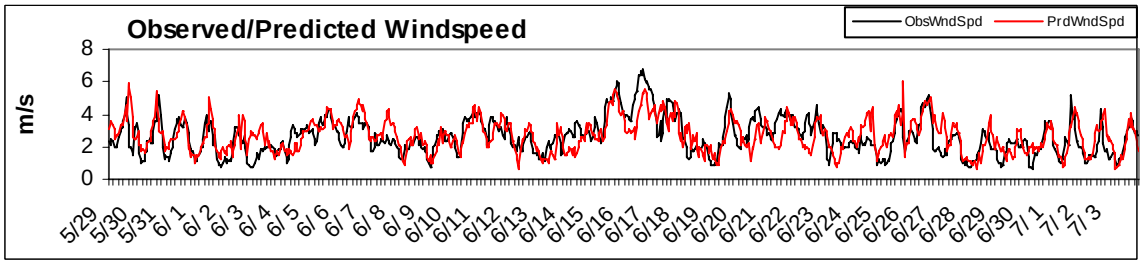

Figure 3-6. Austin area wind speed time series.

TLM 12 km

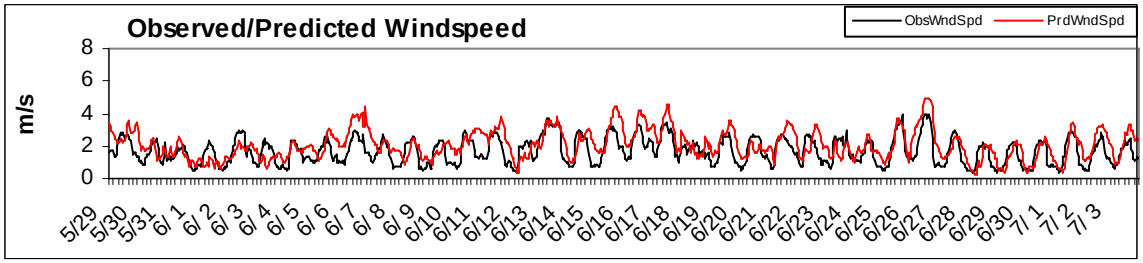

TLM 4 km

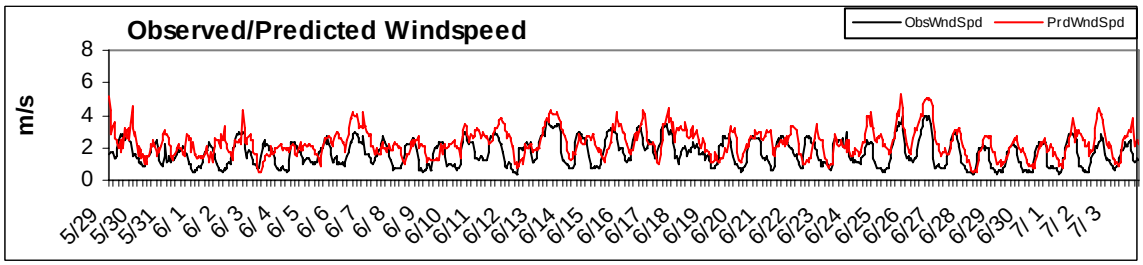

Figure 3-7. Tyler-Longview-Marshall area wind speed time series.

DFW 12 km

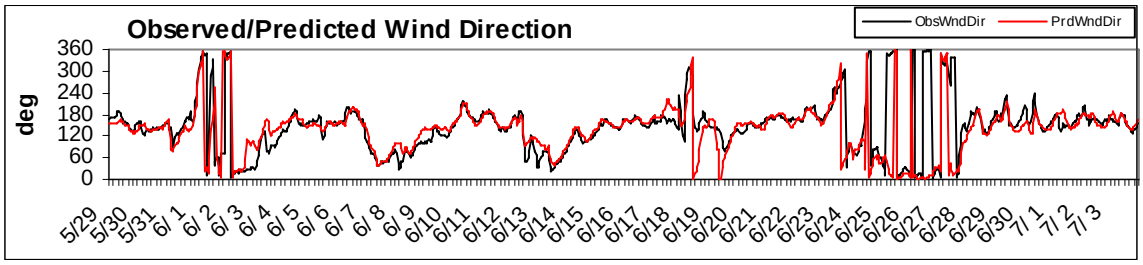

DFW 4 km

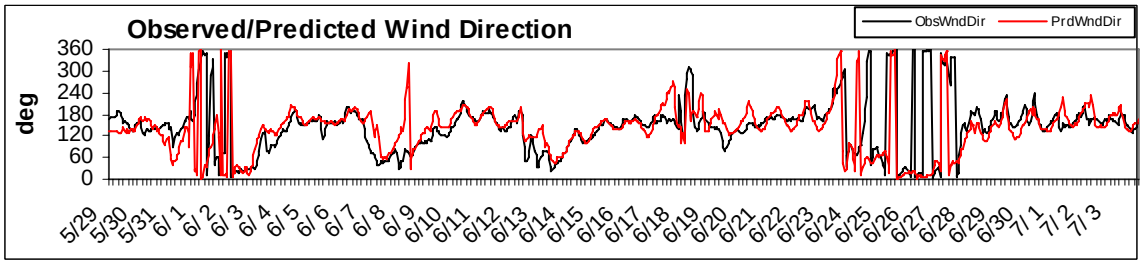

Figure 3-8. DFW wind direction time series.

SA 12 km

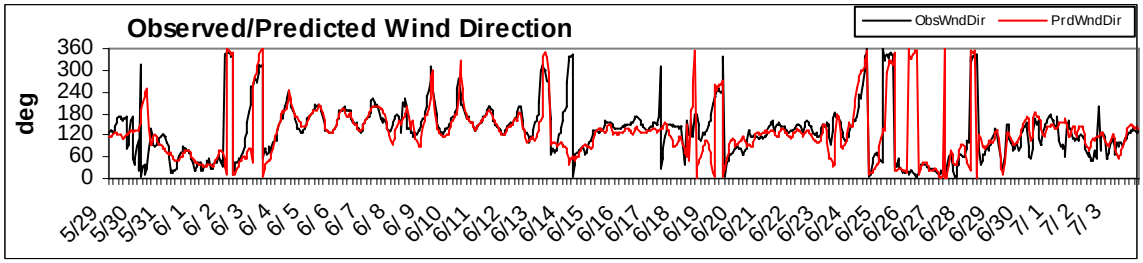

SA 4 km

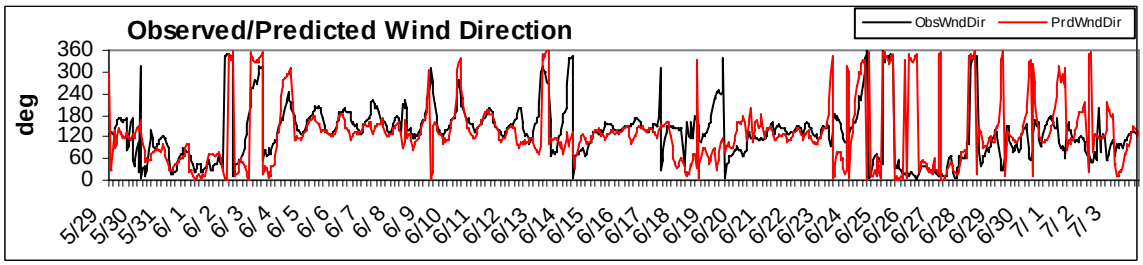

Figure 3-9. San Antonio wind direction time series.

AUS 12 km

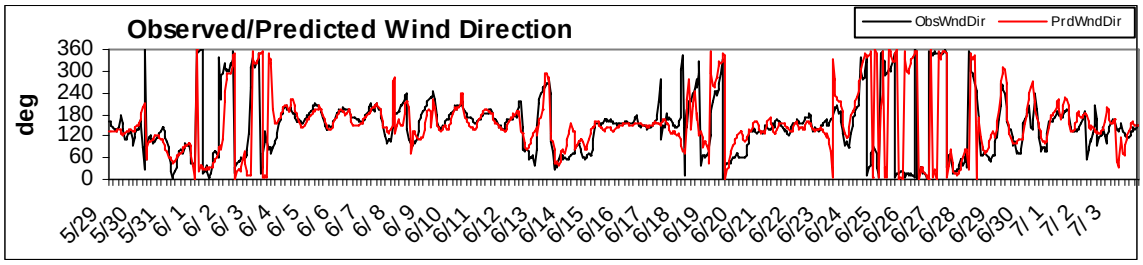

AUS 4 km

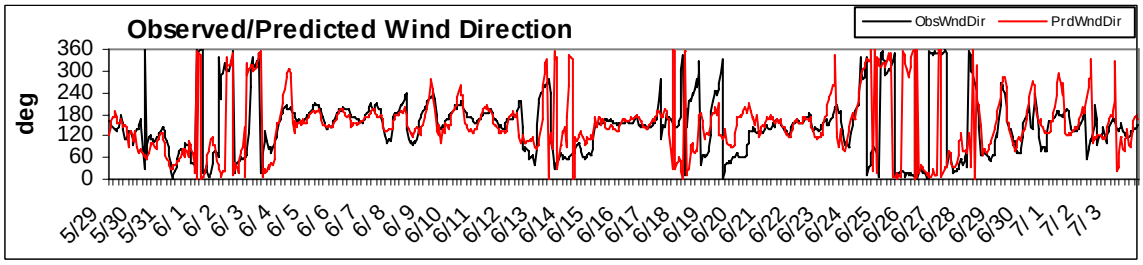

Figure 3-10. Austin wind direction time series.

TLM 12 km

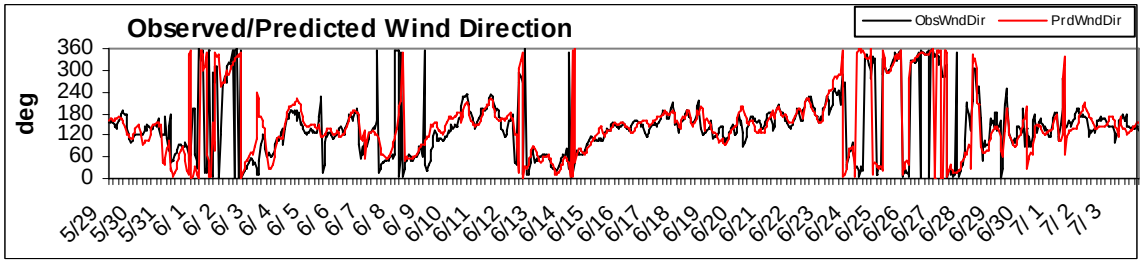

TLM 4 km

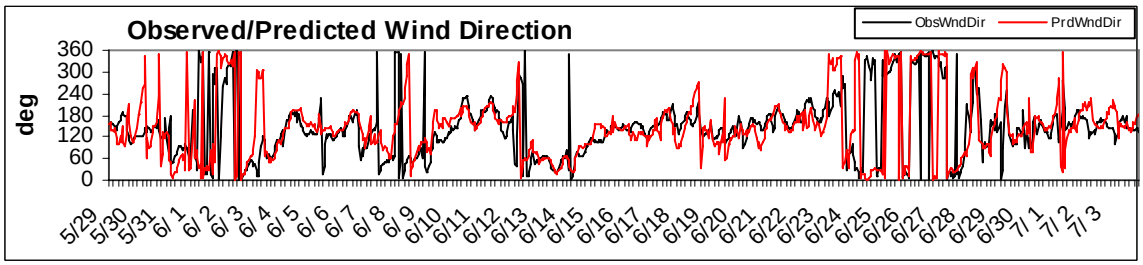

Figure 3-11. Tyler-Longview-Marshall wind direction time series.

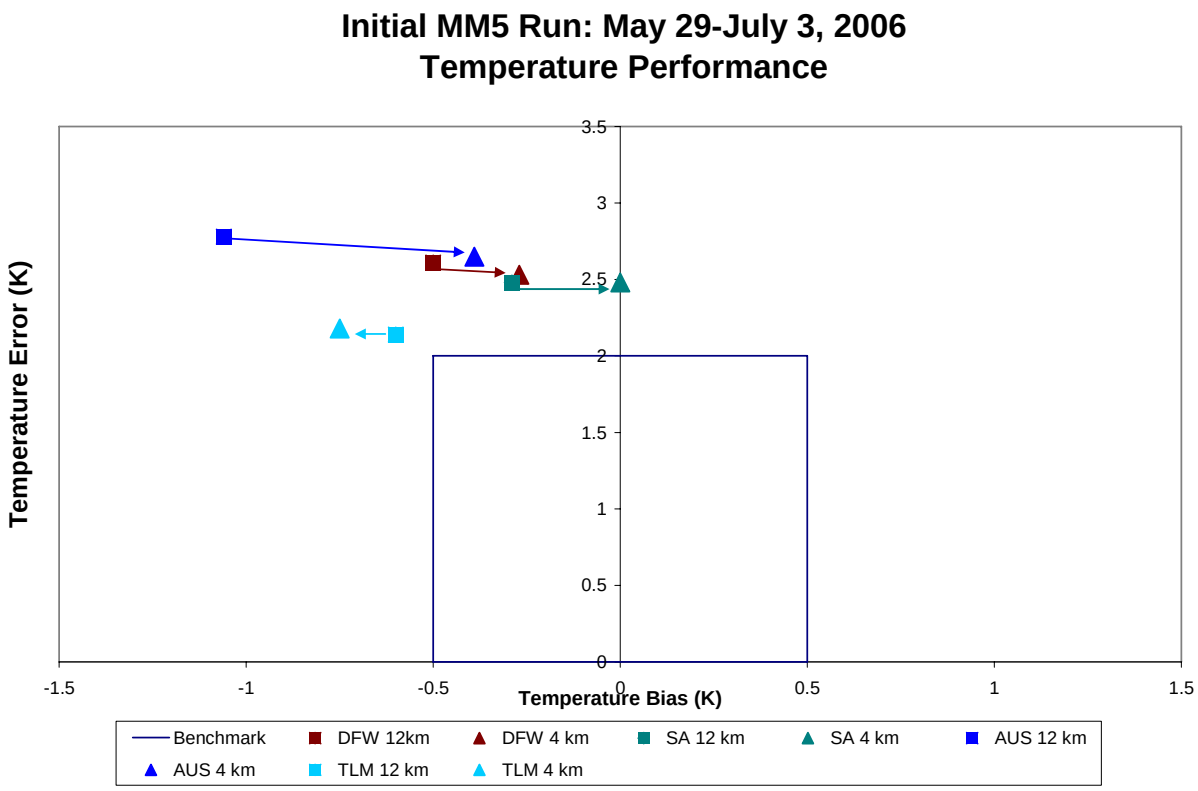

Figure 3-12. Temperature performance soccer plot. Arrows indicate change in performance in going from 12 km grid to 4 km grid.

DFW 12 km

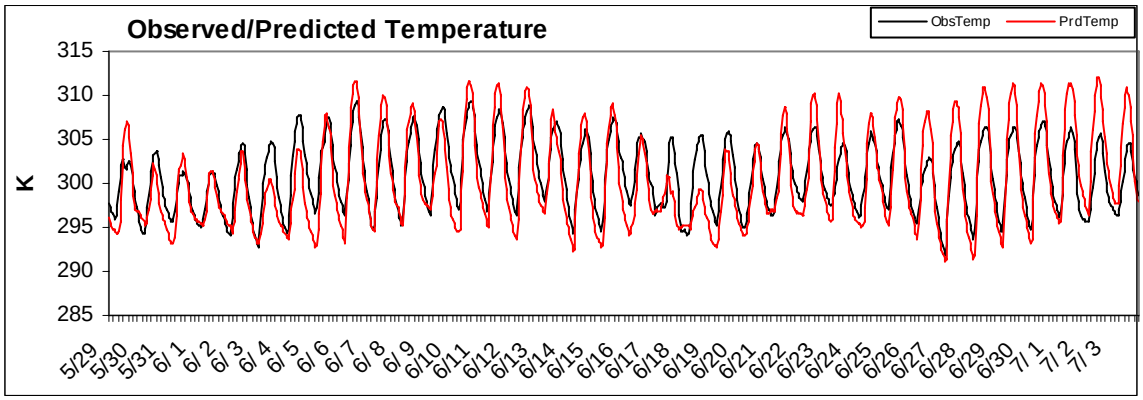

DFW 4 km

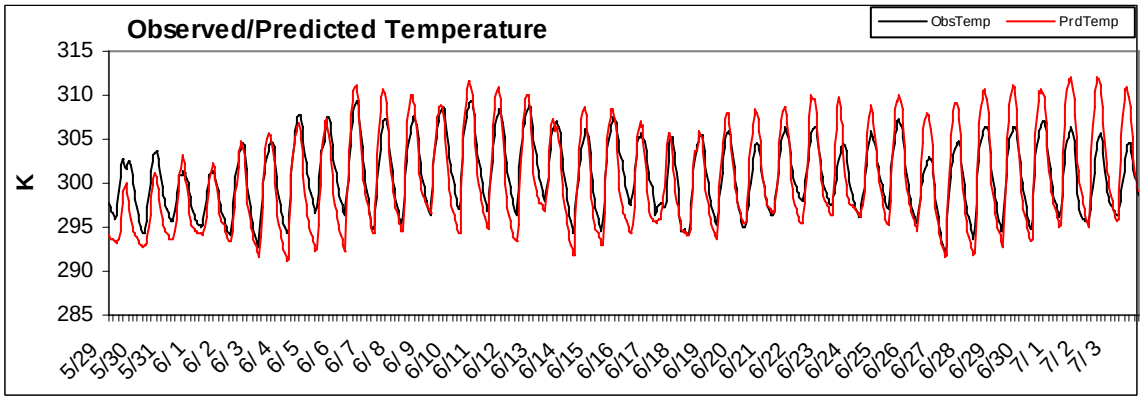

Figure 3-13. DFW area temperature time series.

SA 12 km

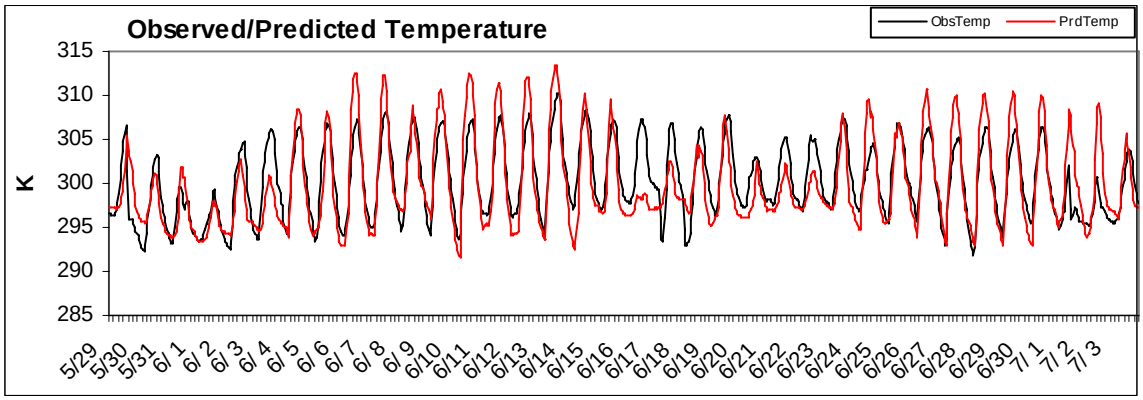

SA 4 km

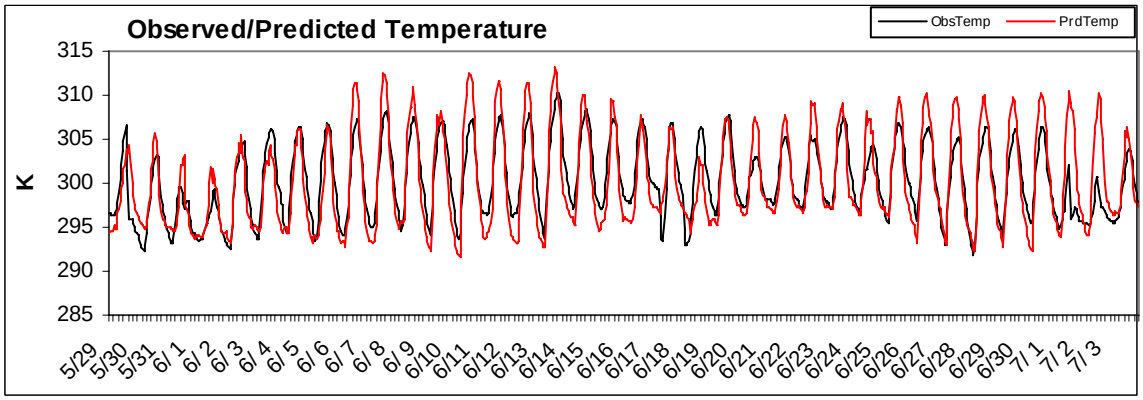

Figure 3-14. San Antonio area temperature time series.

AUS 12 km

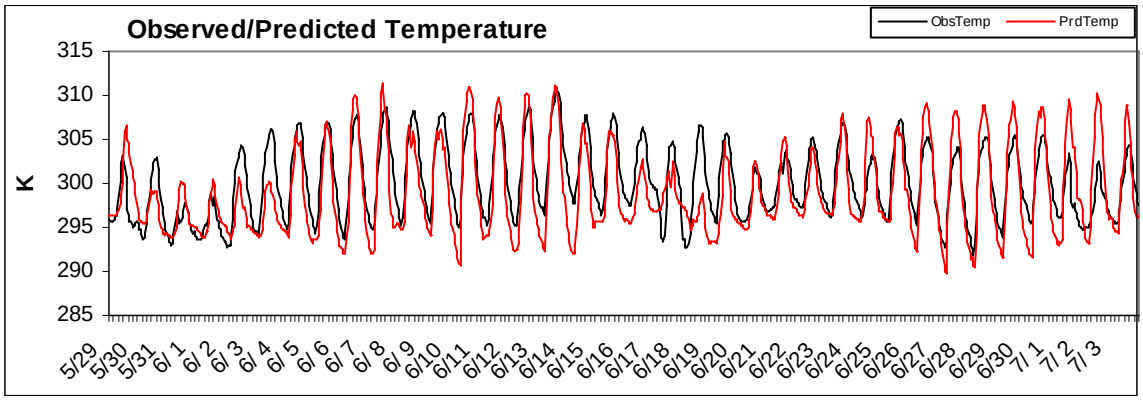

AUS 4 km

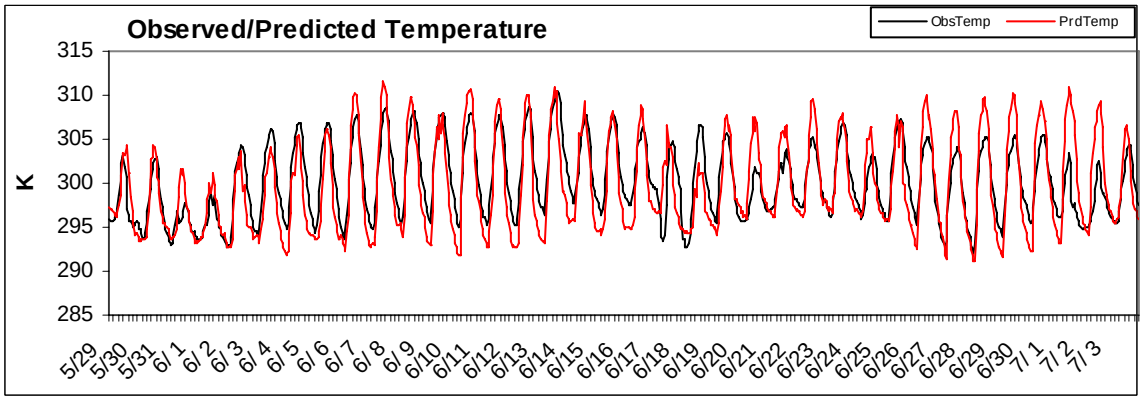

Figure 3-15. Austin area temperature time series.

TLM 12 km

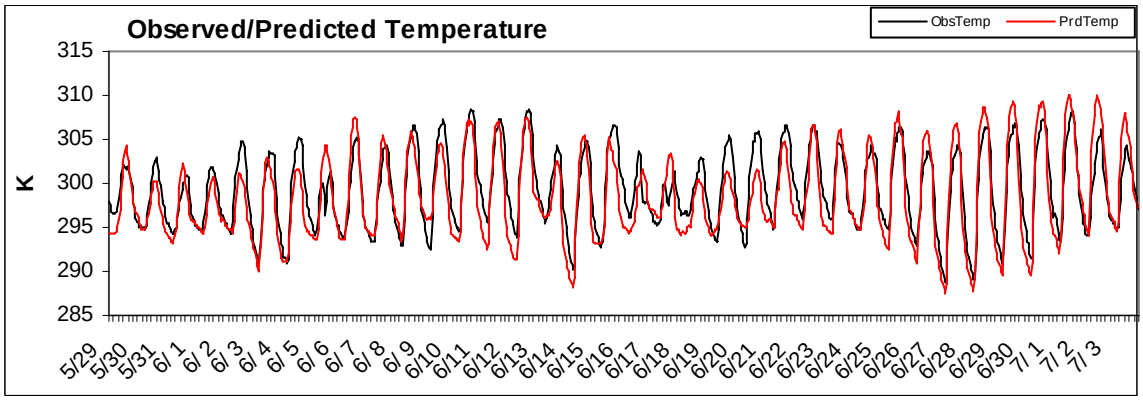

TLM 4 km

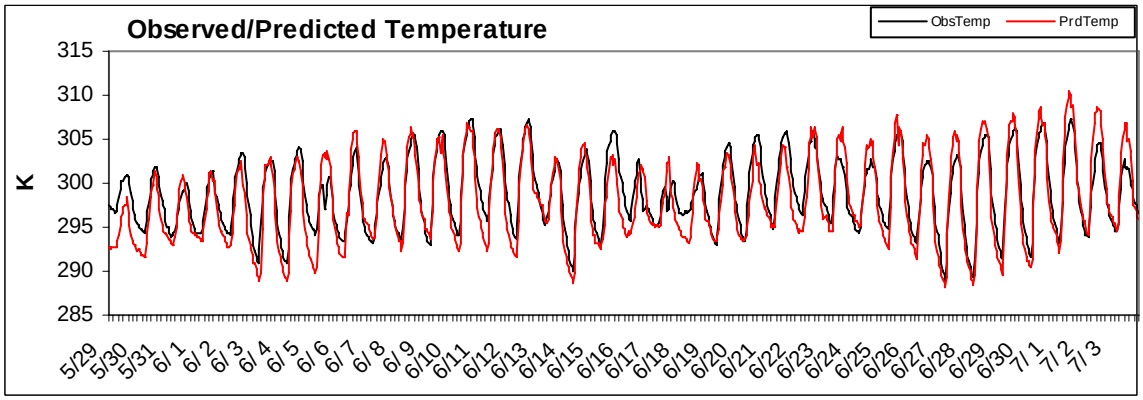

Figure 3-16. Tyler-Longview-Marshall area temperature time series.

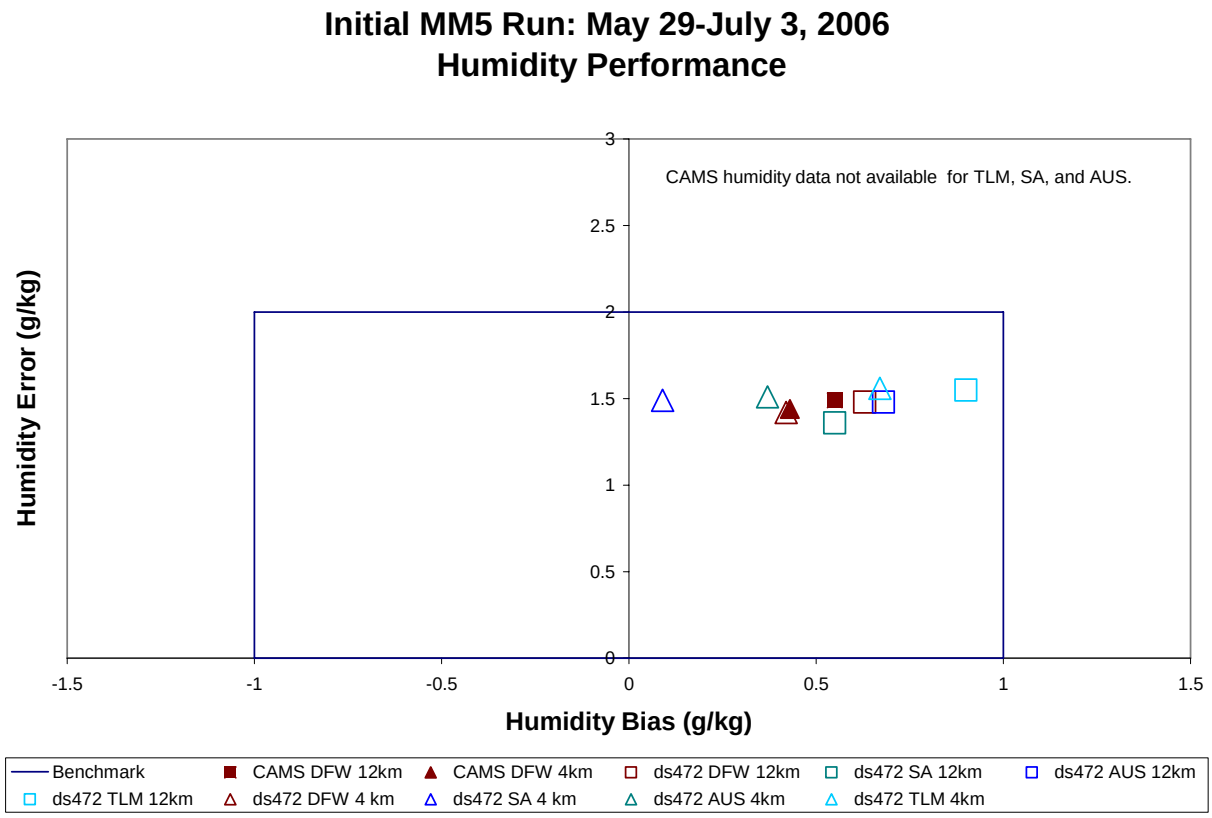

Figure 3-17. Humidity performance soccer plot.

DFW 12 km

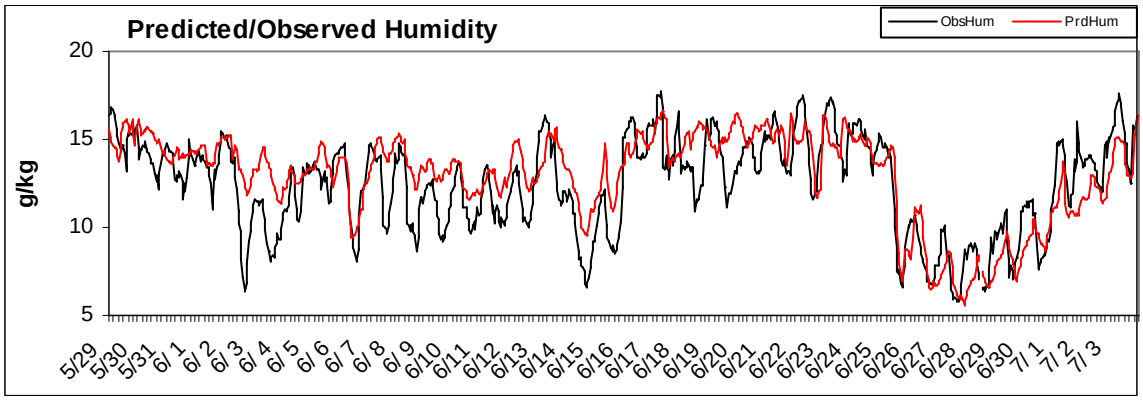

DFW 4 km

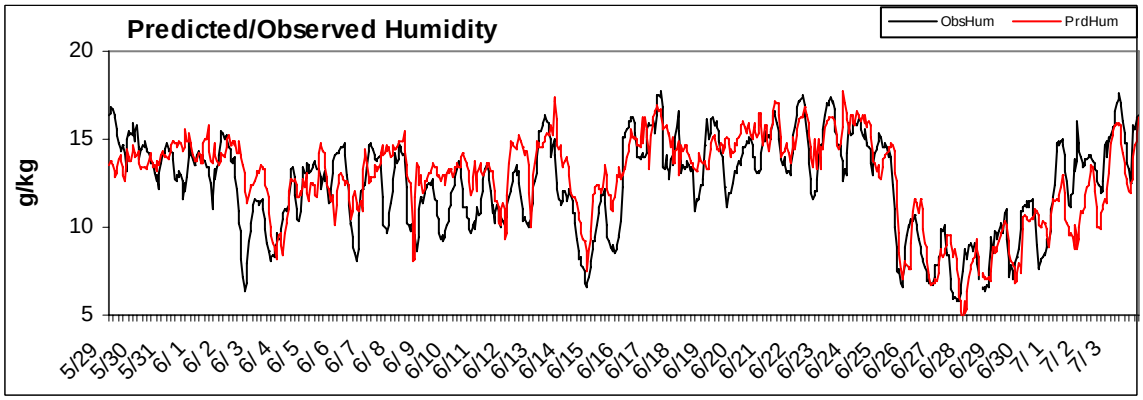

Figure 3-18. DFW area humidity time series.

SA 12 km

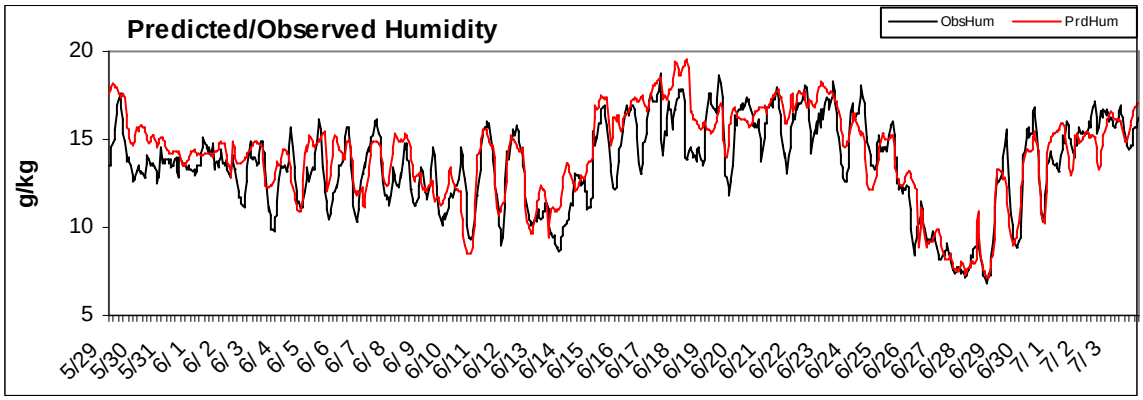

SA 4 km

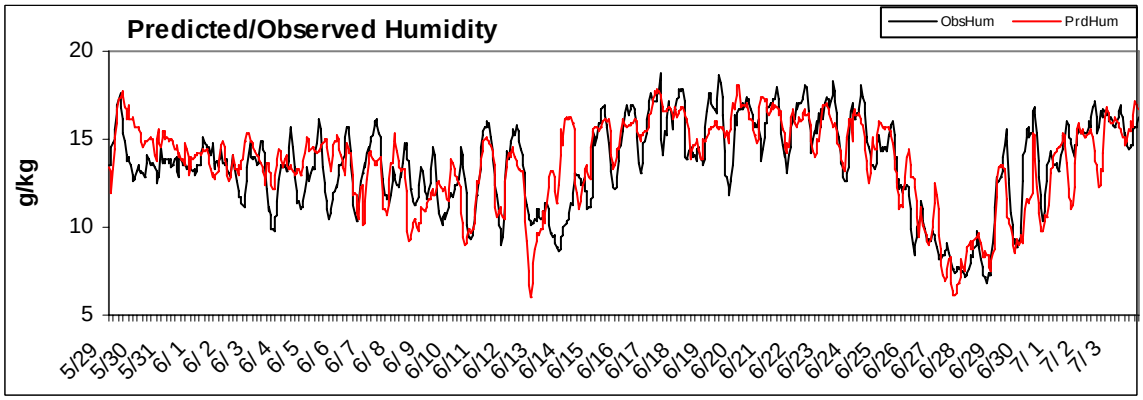

Figure 3-19. San Antonio area humidity time series.

AUS 12 km

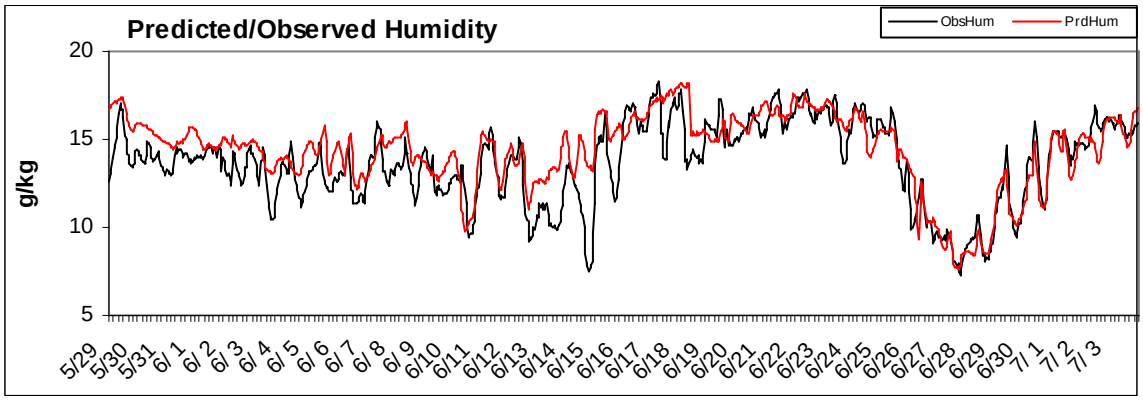

AUS 4 km

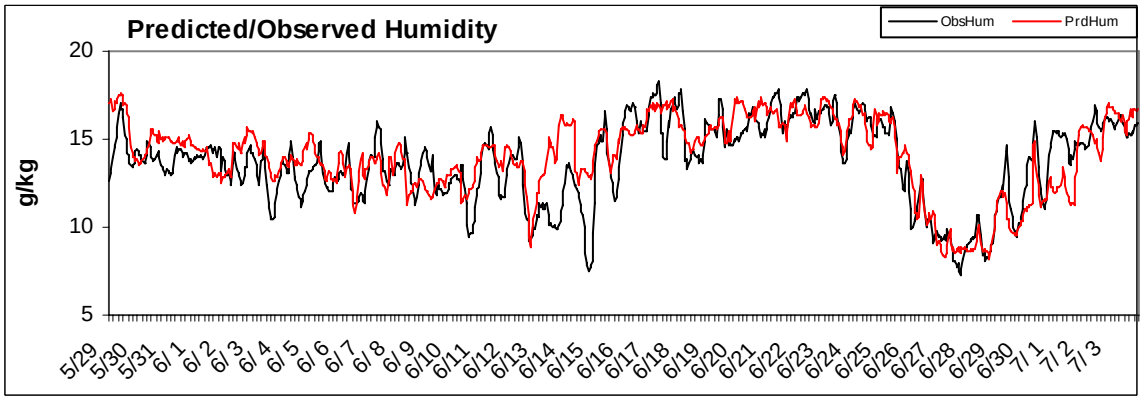

Figure 3-20. Austin area humidity time series.

TLM 12 km

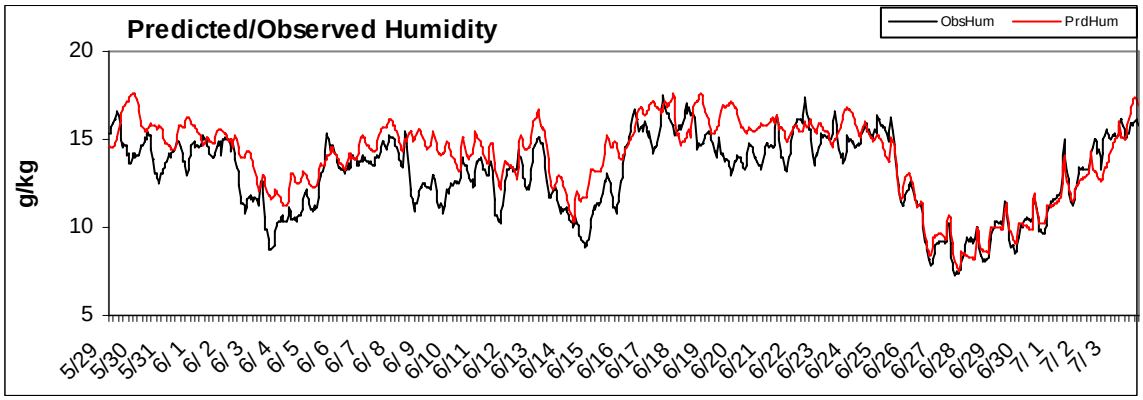

TLM 4 km

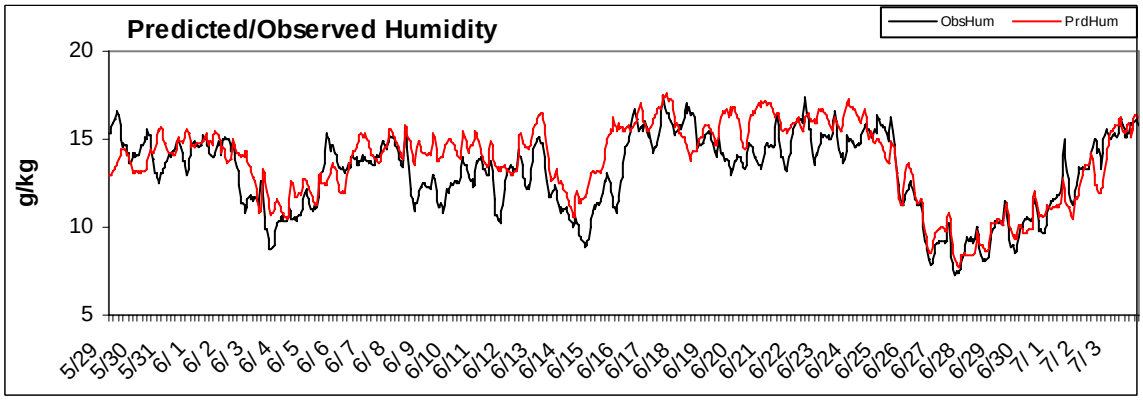

Figure 3-21. Tyler-Longview-Marshall area humidity time series.

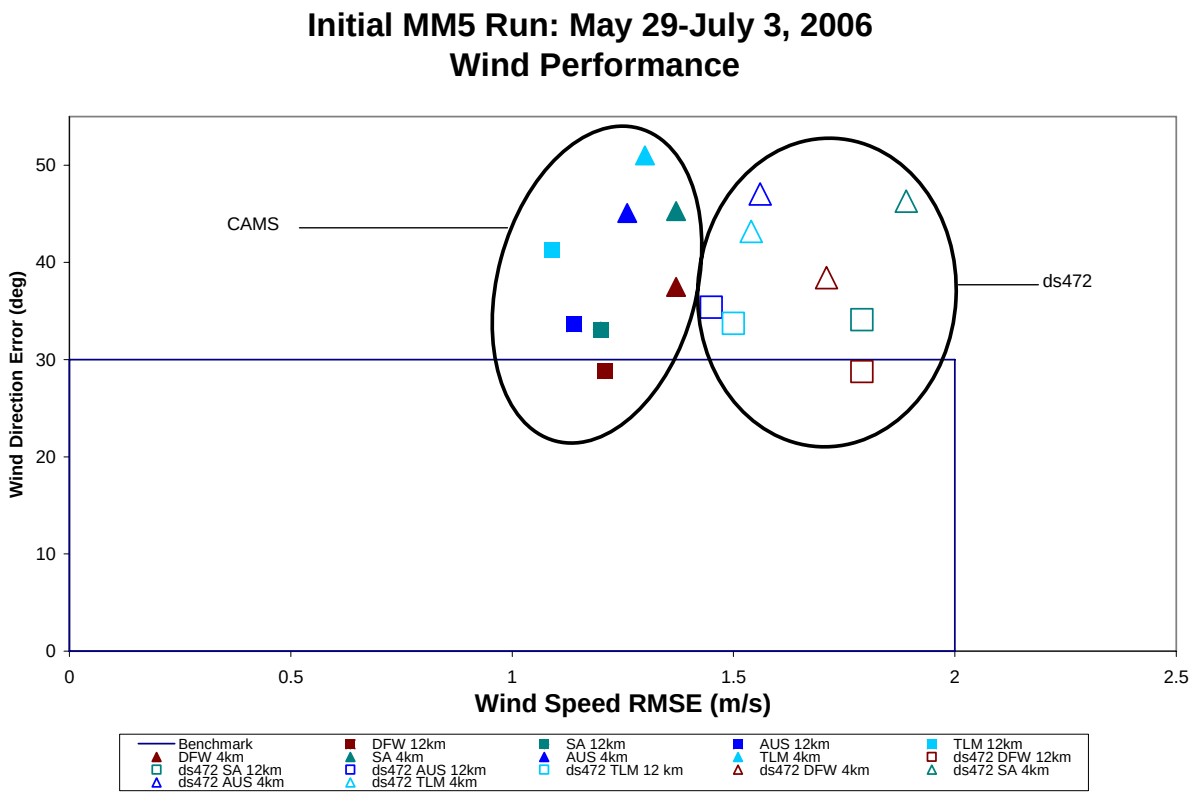

Figure 3-22. Wind performance soccer plot in which evaluation is performed using both CAMS and ds472 datasets.

DFW

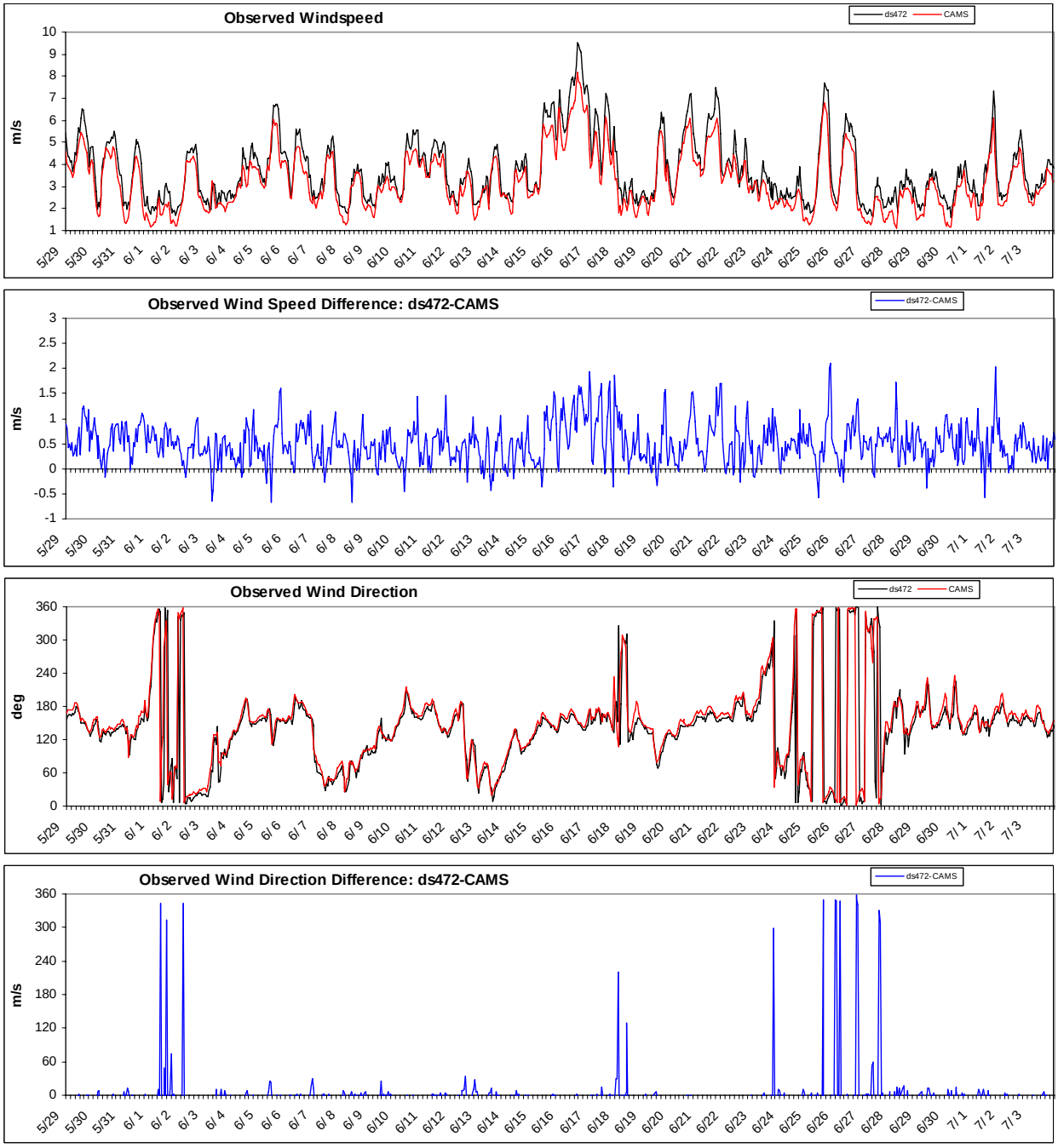

Figure 3-23. Top two panels: wind speed time series for DFW area ds472 (black) and CAMS (red) monitors and difference (blue). Bottom two panels: wind direction time series for DFW area ds472 (black) and CAMS (red) monitors and difference (blue).

4. PRECIPITATION EVALUATION

For each day of the episode, fields of observed precipitation were compared with model total (resolved + convective) rainfall fields on the 12 km and 4 km grids. The observed precipitation amounts were derived from the Climate Prediction Center (CPC) gridded precipitation amount dataset, which is available from the National Weather Service's Climate Prediction Center at http://www.cpc.ncep.noaa.gov/products/precip/realtime/retro.html. The CPC daily precipitation amounts are derived from rain gauge data from the River Forecast Center, and are gridded on a latitude-longitude mesh that covers the U.S. mainland at a resolution of 0.25°x 0.25° (about 25 km x 25 km for Texas in the present modeling domain). The gridded precipitation fields are ramped down to zero immediately offshore of the Continental U.S. The CPC dataset was interpolated to the 12 km MM5 Lambert conformal grid for the analysis presented below.

The advantage of the CPC precipitation data set is that it is a gridded field with reasonably high resolution that can be used to qualitatively evaluate model performance over land. However, this CPC product has a very coarse resolution compared to that of the 4 km grid, and features such as intense localized precipitation from thunderstorms will be smoothed out in the CPC fields so that its maxima will be less intense and its rainfall will be distributed over a wider area than in the real world or on the 4 km MM5 grid. This CPC product can be most effectively used as a screening tool to determine whether there was any rainfall in a given area on a particular day, rather than to compare specific rainfall amounts. The CPC data set is therefore useful in diagnosing the presence of anomalous convection.

Episode Total Precipitation Comparison

We begin by examining the episode total rainfall in the CPC observations and on the 12 km and 4 km MM5 grids. The CPC data show a band of enhanced precipitation along the Gulf Coast with maxima near Victoria and northeast of Houston (Figure 4-1, upper panel). This band of precipitation is dramatically less intense in the MM5 12 km grid field (Figure 4-1, lower panel). The model field has its maximum intensity offshore in the Gulf of Mexico. It is not possible to verify this feature using the CPC data set. It is clear, however, that on the 12 km grid, the model underestimates precipitation along the coast and overestimates precipitation in isolated areas of the TLM area and in a band extending from the TLM region southwestward toward the Austin area.

Figure 4-2 shows the episode total rainfall for the 4 km grid and for the area of the 12 km grid that contains the 4 km grid. The CPC observations are interpolated to 12 km resolution, and have been windowed to the 4 km grid; as discussed above, observations are gridded at a much coarser resolution than the model output, and so maxima should be less intense and the precipitation field more diffuse than in the 4 km model prediction. Figure 4-2 shows striking differences between the precipitation patterns on the 12 km and 4 km grids. Precipitation on the 4 km grid tends to be confined to smaller areas and to have higher maxima, while precipitation tends to occur over a larger area on the 12 km grid, and to have lower maxima. This effect goes beyond what might be expected from the smoothing due to the lower resolution of the 12 km grid. The envelope of the rainfall pattern on the 4 km grid more closely approximates the observations than does the pattern on the 12 km grid. In the 4 km grid field, a band of

precipitation lies inland of and parallel to the coast, although there are also regions of precipitation that do not appear in the observations, such as the region of high total precipitation seen over Northern Louisiana on the 4 km grid.

On the 12 km grid, then, there is generally too little rainfall over the Gulf Coast in the episode average, with MM5 missing the observed maximum precipitation region along the Texas Coast. On the 4 km grid, there is more precipitation in this region than on the 12 km grid in the Houston-Galveston and Victoria areas, although MM5 underestimates rainfall over much of the coastal region. Away from the coastal maximum, MM5 tends to overpredict rainfall in the Waco area and in Northern Louisiana on the 4 km grid. There are pockets of intense localized rainfall where little observed rain fell throughout the 4 km domain, and this may indicate the presence of anomalous convection.

The differences in the character of the rainfall fields on the 4 km and 12 km grids are due in part to the difference in resolution, but are also likely related to the fact that the Grell cumulus parameterization was used on the 12 km grid, but no cumulus parameterization was used on the 4 km grid. When no cumulus parameterization is used, the cloud microphysics scheme and core model dynamics explicitly simulate convection. Molinari and Dudek (1992) have shown that the explicit simulation of convection in mesoscale models can cause an unphysical phase delay in the onset of convective rainfall because condensation cannot occur until the model becomes saturated at the resolved grid scale. In the real world, saturation occurs on a scale that may be smaller than the model grid resolution; in a parameterization, the cloud model must saturate the column, but the grid need not be saturated. When a cumulus parameterization is used, therefore, instability is likely to be released sooner, as convection is triggered before grid scale instability is allowed to build up. This can cause marked differences in the rainfall pattern in a simulation that incorporates a cumulus parameterization relative to one that does not. Cumulus parameterization tends to reduce the frequency of occurrence of intense localized convection and increase the areal coverage of less intense rainfall in the simulation with the cumulus parameterization. This is consistent with the 12 km and 4 km grid precipitation fields from this simulation, as can be seen from Figure 4-2 as well as the daily precipitation plots discussed below.

Daily Total Precipitation Comparison

For rainy periods during the May 29-July 3, 2006 episode, daily total observed and modeled precipitation amounts were compared, with an emphasis on identifying regions where anomalous convection may have occurred in the model. Figures 4-3 through 4-9 show observed and modeled precipitation on the 12 km and 4 km grids. As in Figure 4-2, the CPC and 12 km grid precipitation fields are windowed to show only the 4 km grid region.

During the period May 31-June 2 (Figure 4-3), MM5 overestimates precipitation over most of the domain. The overestimate is especially pronounced in North Central Texas on the 12 km domain, where widespread weak rainfall is found in regions where the observed precipitation field is dry. Inspection of the DFW 12 km grid humidity time series (Figure 3-18) shows that the model has a wet bias during the May 31-June 2 period. This wet bias is smaller for the 4 km grid, on which the areal extent of precipitation is generally smaller during this period. Regions of possible anomalous convection may be identified on each day. Of particular note are the large

area of intense rain on the 4 km grid on May 29, and, on May 29-June 1, bands of rainfall oriented from north to south in Louisiana, and pockets of rain along the Gulf Coast on the 4 km grid. Performance improved by June 2, with the model doing a better job of reproducing the observed rainfall pattern on both grids on June 2, and the incidence of anomalous convection reduced on the 4 km grid. By June 4, most of the domain was free of rain.

During the period June 6-8 (Figure 4-4), rain extended southward along the Texas-Louisiana border. MM5 underestimated the areal extent of the observed rainfall, and may have overestimated the maximum intensity (June 6 on the 12 km grid and June 7 on the 4 km grid). June 9 is included in Figure 4-4. Although this was not a when rain was observed, it is a high ozone day in DFW and Houston.

During the period June 13-June 16, the CPC precipitation field shows that much of the domain remained dry (Figure 4-5). The model overestimates the precipitation during this period. On June 13, for example, the observations show precipitation in Arkansas, but there is precipitation over a large area of Texas in both the 12 km and 4 km simulations. On June 14, the CPC field shows precipitation in the Houston area. On the 12 km grid, the model displaced the precipitation to the southwest. On the 4 km grid, the precipitation maximum is located further northeast than on the 12 km grid, and its highly localized spatial signature suggests the presence of anomalous convection. Anomalous convection on June 13-14 will be discussed further in the next section. On June 15, the model overestimates precipitation on the 4 km grid, and on June 16, there is more rain on both grids than in the observations, with strong maxima on the 4 km grid near Houston suggesting the presence of anomalous convection.

By June 17, Texas had entered a rainy period during which daily maximum 8-hour ozone values fell below 80 ppb (Figure 1-1), except in DFW. From June 17-25, rain appears in the observations. The signature of apparent anomalous convection is present on the 4 km grid on June 17-19.

During June 26-July 1, there is little or no precipitation in the regions of interest (Figure 4-9), and the second period of elevated ozone concentrations is underway (Figure 1-1). During this time, the MM5 humidity performance improved, with a more realistic simulation of the diurnal cycle in humidity than is seen earlier in the simulation (Figures 3-18 through 3-21).

Precipitation Evaluation Summary

- Precipitation on the 4 km grid tends to be confined to smaller areas and to have higher maxima, while precipitation tends to occur over a larger area on the 12 km grid, and to have lower maxima.

- Observed daily precipitation totals were not well simulated by the model on either the 12 km or the 4 km grid.

- The episode total precipitation pattern over Texas was reproduced with greater fidelity on the 4km grid than on the 12 km grid.

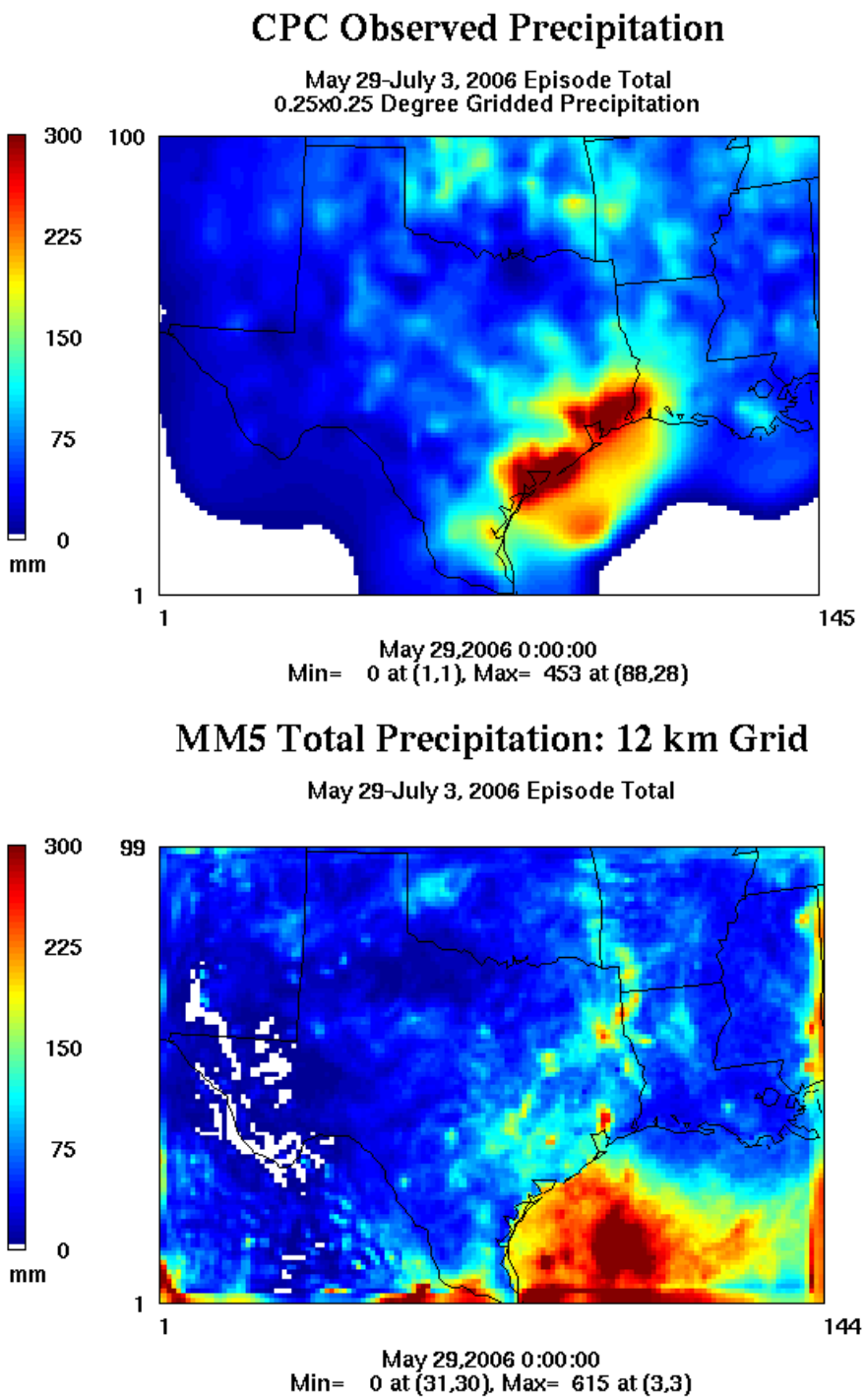

Figure 4-1. Episode precipitation totals (mm). Top panel: CPC observed precipitation. Bottom panel: MM5 precipitation on the 12 km grid.

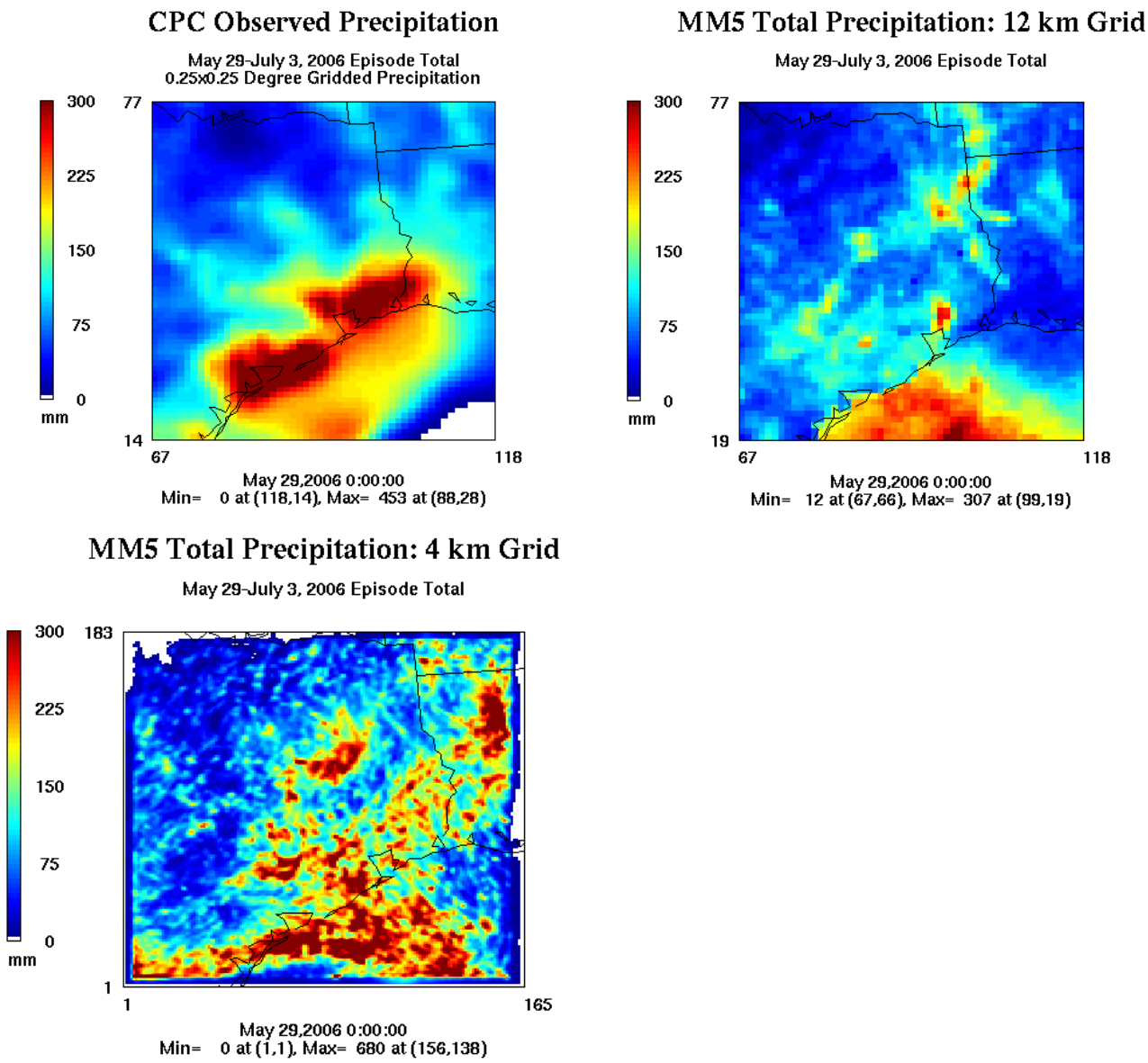

Figure 4-2. Episode precipitation totals (mm). Top left panel: CPC observed precipitation in the region spanned by the 4 km grid. Top right panel: MM5 precipitation on the 12 km grid in the 4 km grid region. Lower left panel: MM5 precipitation on the 4 km grid.

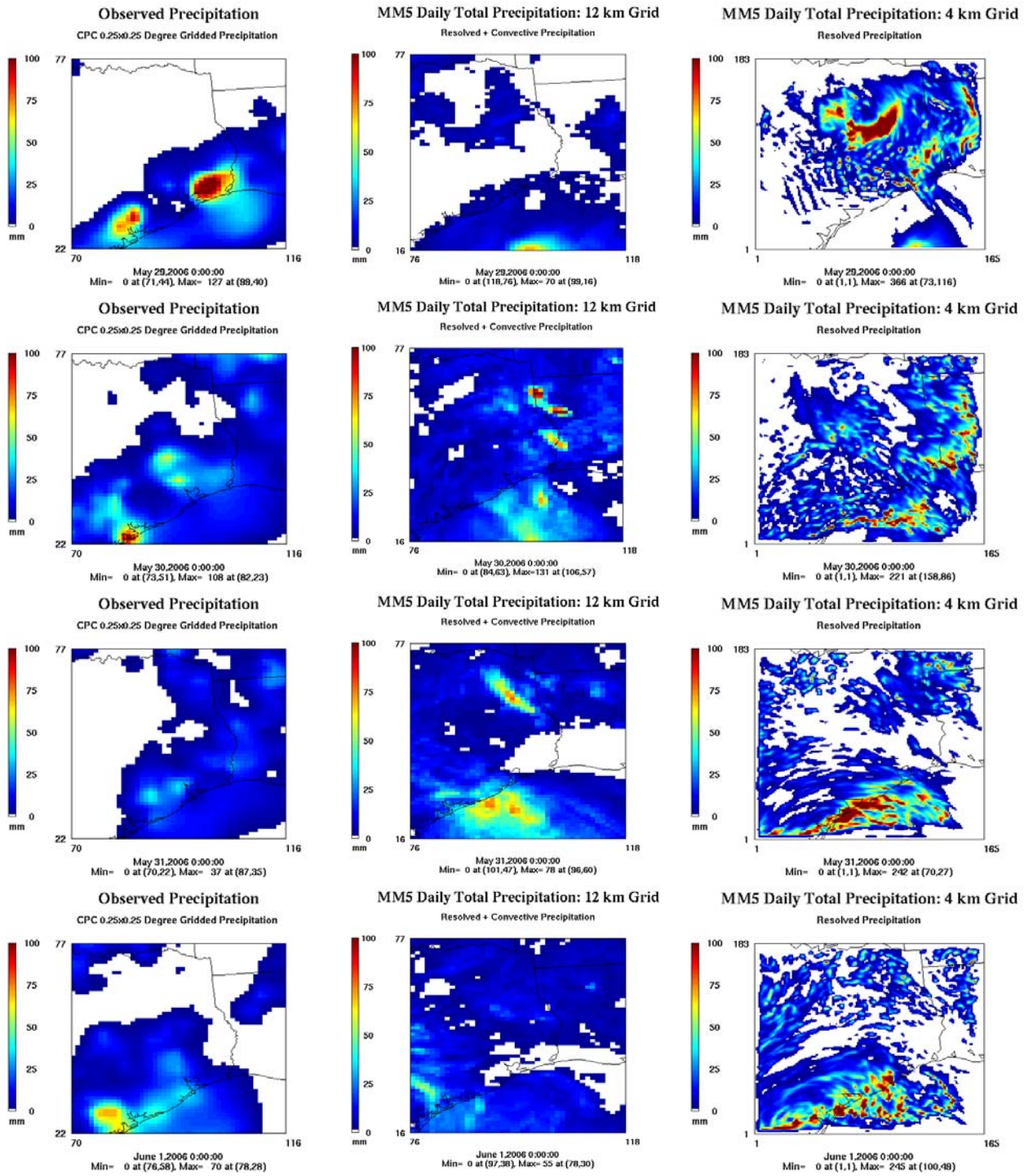

Figure 4-3. Daily precipitation totals (mm) for May 29-June 1, 2006. Left hand column: CPC observed precipitation in the region spanned by the 4 km grid. Center column: MM5 precipitation on the 12 km grid in the 4 km grid region. Right hand column: MM5 precipitation on the 4 km grid.

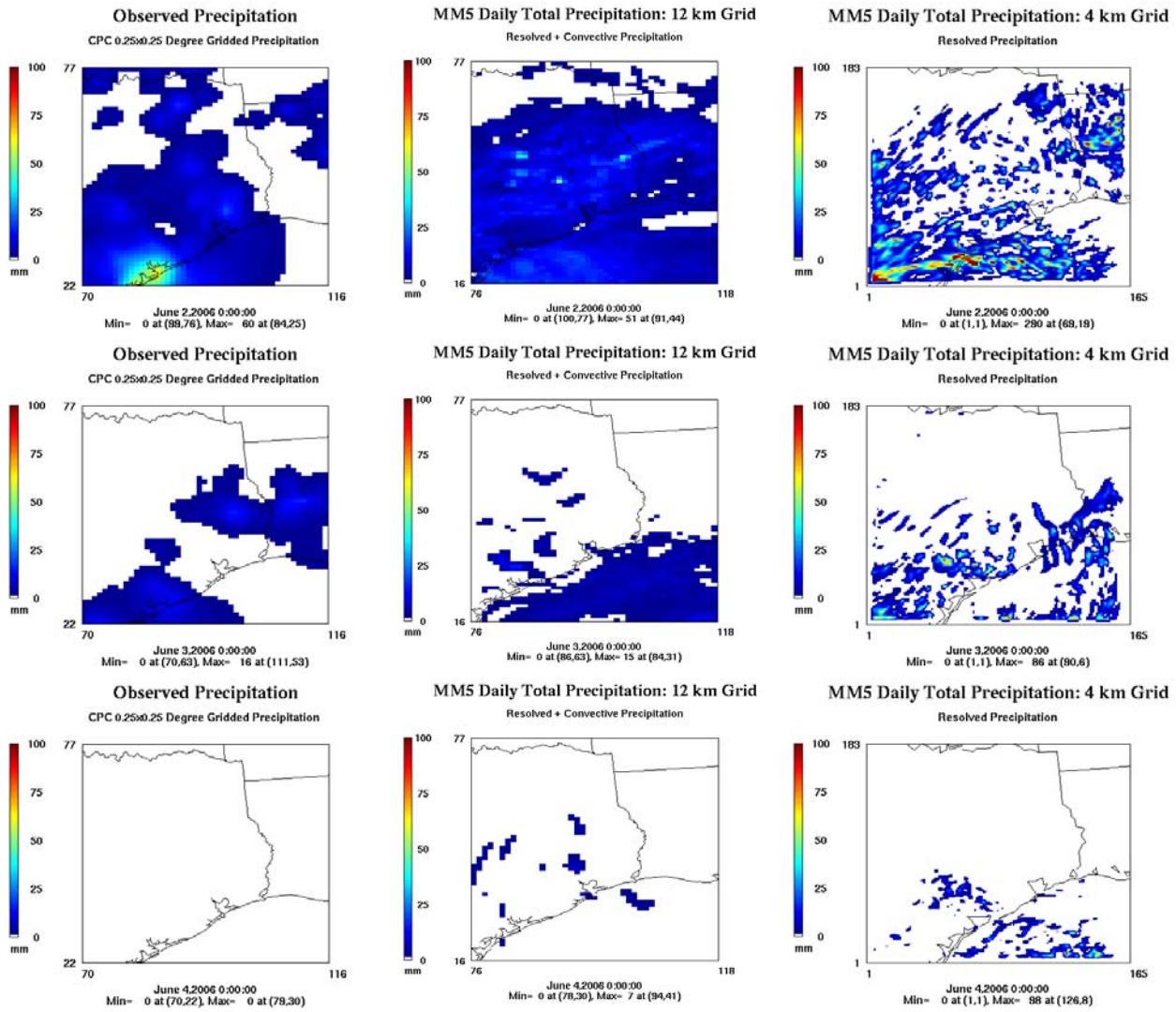

Figure 4-3 (continued). Daily precipitation totals (mm) for June 2-4, 2006. Left hand column: CPC observed precipitation in the region spanned by the 4 km grid. Center column: MM5 precipitation on the 12 km grid in the 4 km grid region. Right hand column: MM5 precipitation on the 4 km grid.

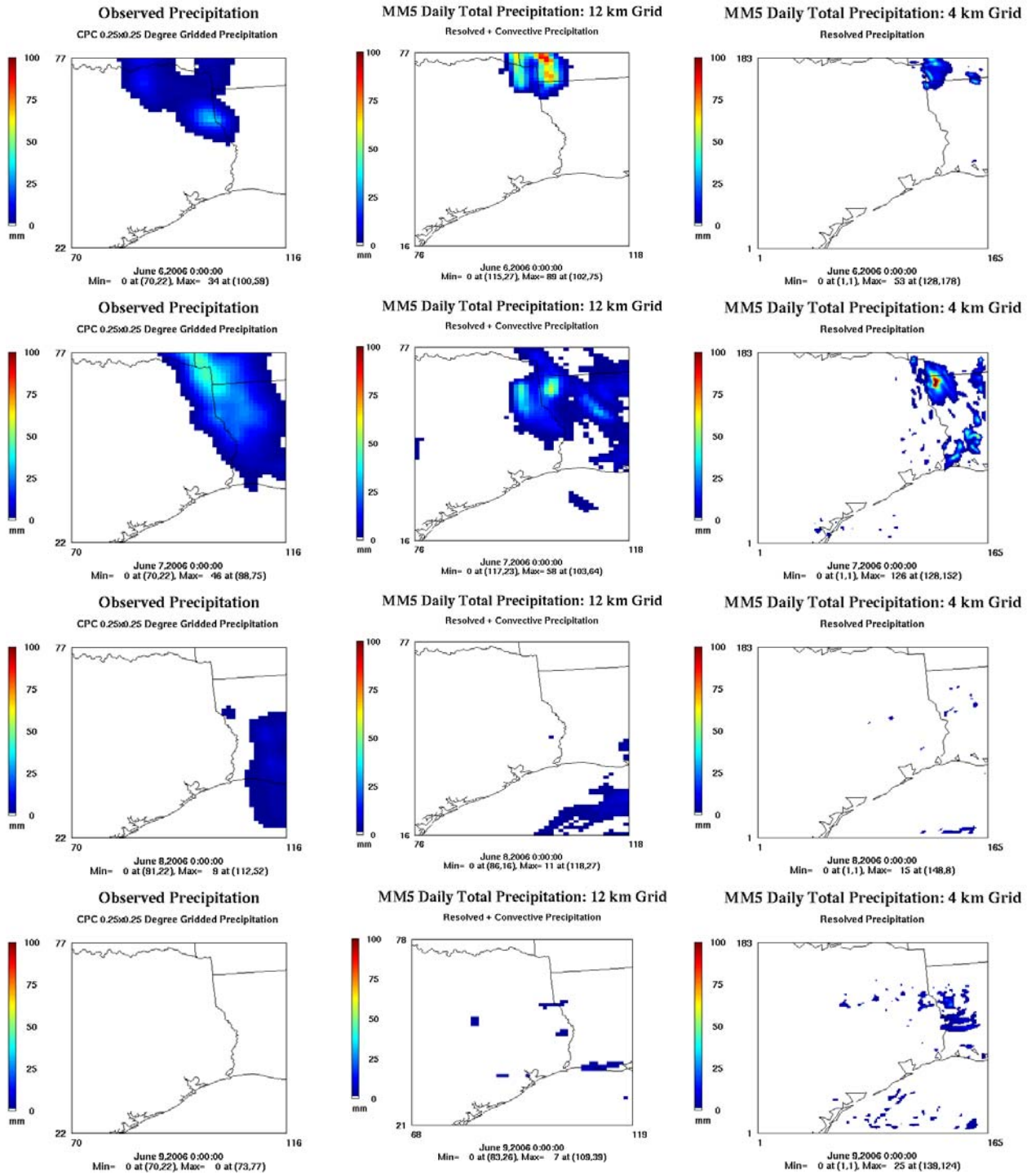

Figure 4-4. Daily precipitation totals (mm) for June 6-9, 2006. Left hand column: CPC observed precipitation in the region spanned by the 4 km grid. Center column: MM5 precipitation on the 12 km grid in the 4 km grid region. Right hand column: MM5 precipitation on the 4 km grid.

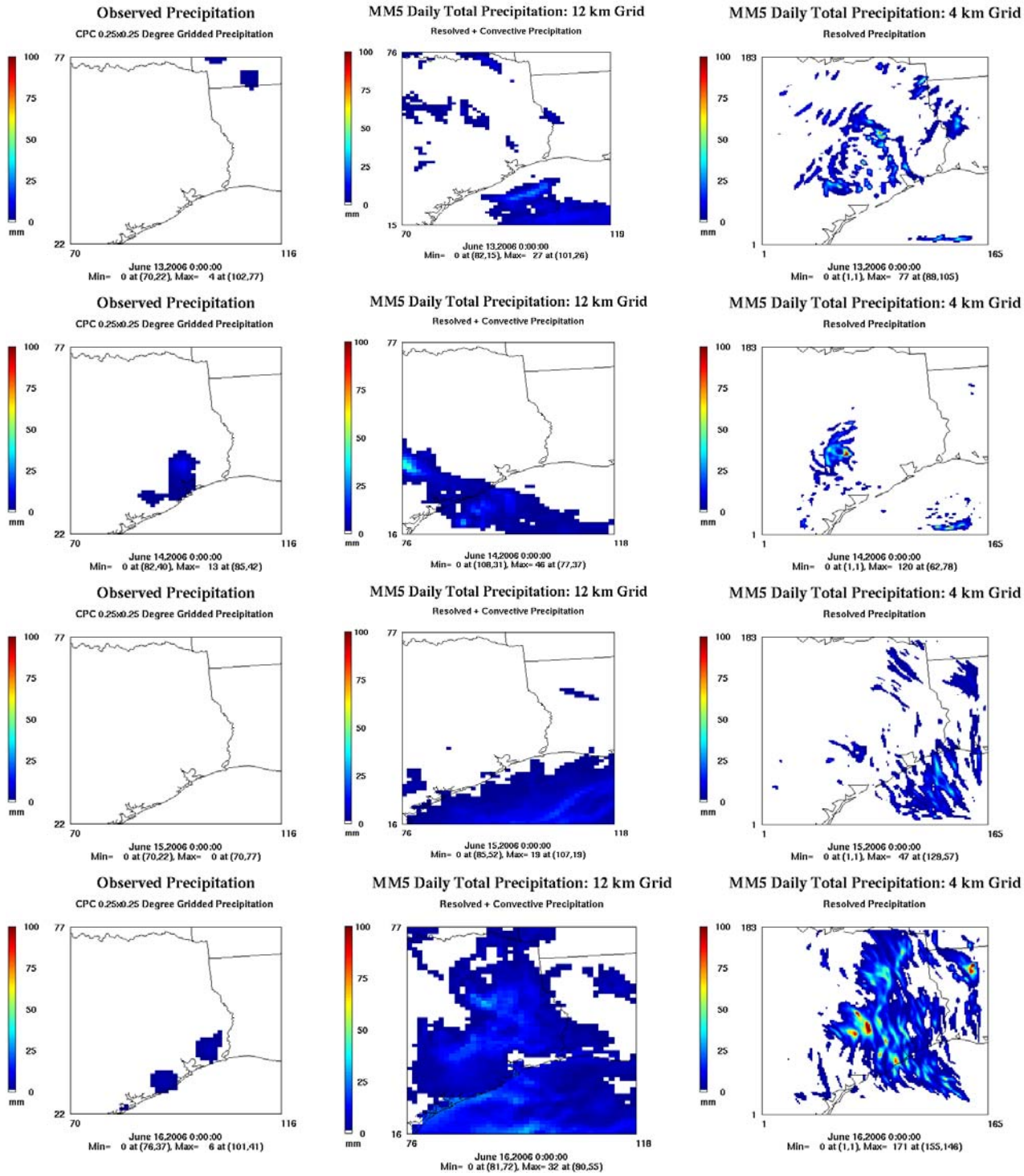

Figure 4-5. Daily precipitation totals (mm) for June 13-16, 2006. Left hand column: CPC observed precipitation in the region spanned by the 4 km grid. Center column: MM5 precipitation on the 12 km grid in the 4 km grid region. Right hand column: MM5 precipitation on the 4 km grid.

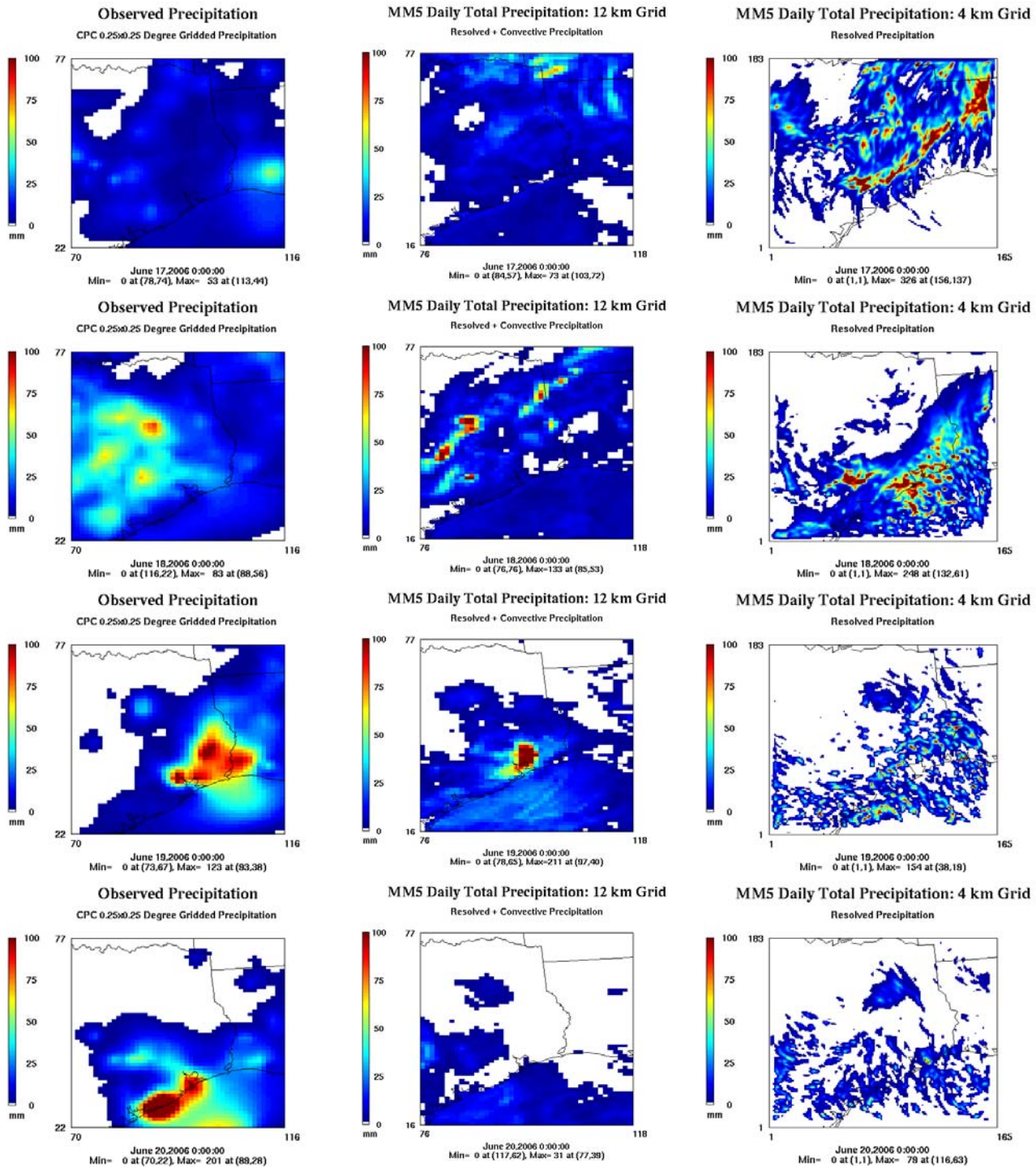

Figure 4-6. Daily precipitation totals (mm) for June 17-20, 2006. Left hand column: CPC observed precipitation in the region spanned by the 4 km grid. Center column: MM5 precipitation on the 12 km grid in the 4 km grid region. Right hand column: MM5 precipitation on the 4 km grid.

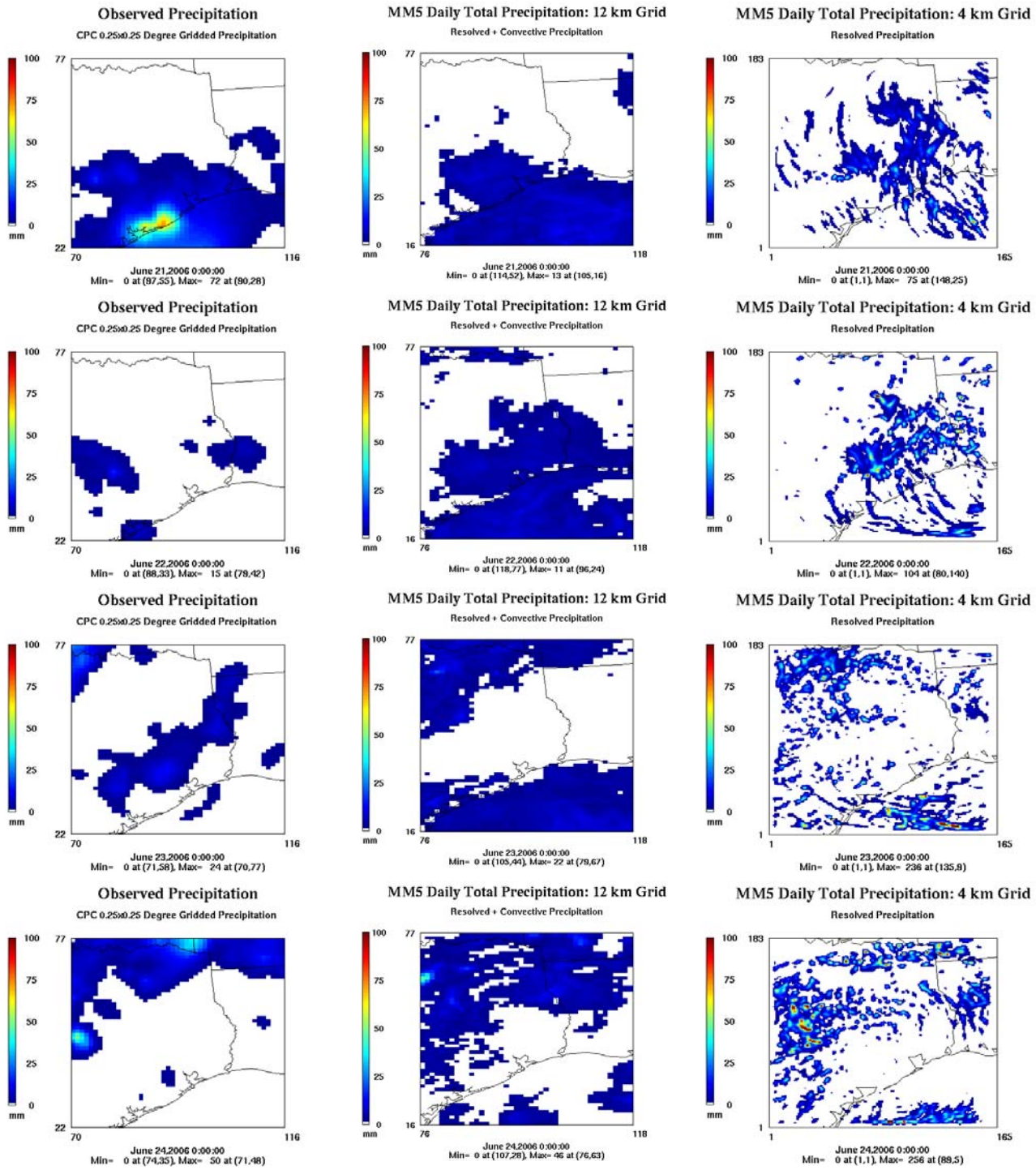

Figure 4-7. Daily precipitation totals (mm) for June 21-24, 2006. Left hand column: CPC observed precipitation in the region spanned by the 4 km grid. Center column: MM5 precipitation on the 12 km grid in the 4 km grid region. Right hand column: MM5 precipitation on the 4 km grid.

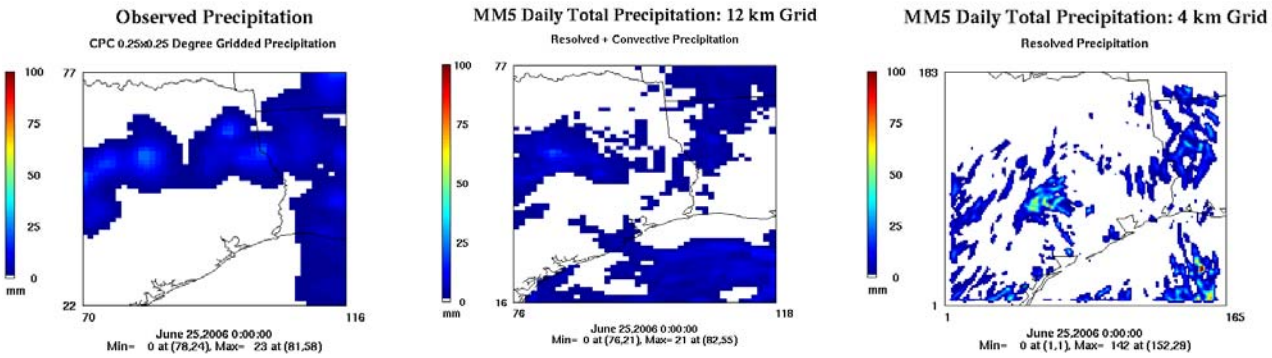

Figure 4-8. Daily precipitation totals (mm) for June 25, 2006. Left hand column: CPC observed precipitation in the region spanned by the 4 km grid. Center column: MM5 precipitation on the 12 km grid in the 4 km grid region. Right hand column: MM5 precipitation on the 4 km grid.

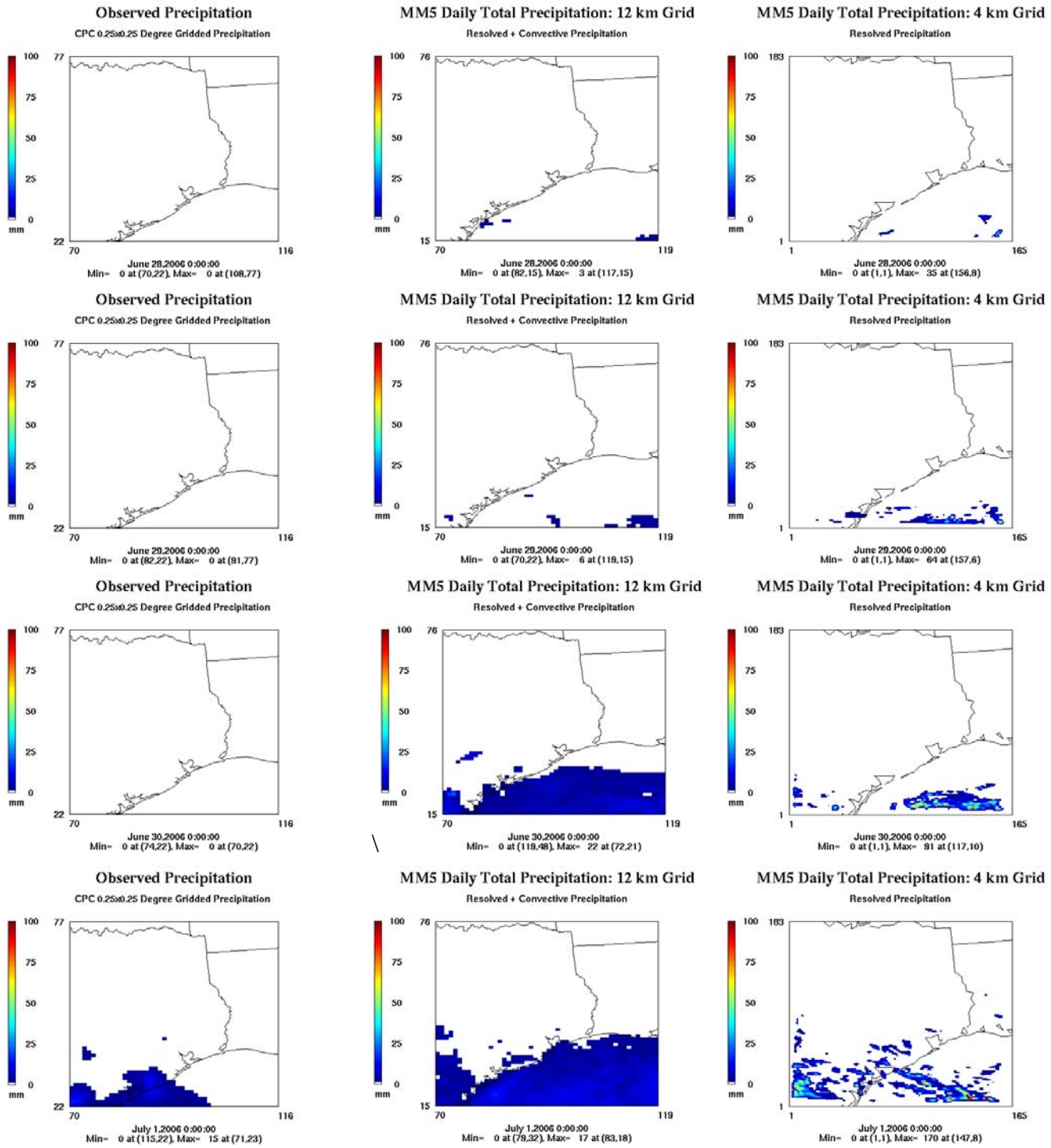

Figure 4-9. Daily precipitation totals (mm) for June 28-July 1, 2006. Left hand column: CPC observed precipitation in the region spanned by the 4 km grid. Center column: MM5 precipitation on the 12 km grid in the 4 km grid region. Right hand column: MM5 precipitation on the 4 km grid.

5. EVALUATION OF PRESENCE OF ANOMALOUS CONVECTION

Comparison of daily average precipitation plots on the 12 km and 4 km grids with the CPC observed fields showed that anomalous convection occurs intermittently throughout the simulation (Figures 4-3 through 4-9). It is possible that wind performance, which is critical for ozone modeling, is affected by this anomalous convection. Convection that is located incorrectly and/or too intense may result in spurious downdrafts that degrade wind speed and direction performance. These downdrafts can also affect temperature and humidity by incorrectly modifying the partitioning of the surface energy flux. Because the focus of any future ozone modeling application involving this MM5 database will be on periods of high ozone, we examined high ozone periods during the May 29-July 3, 2006 episode to determine whether anomalous convection could have affected the model's wind performance. The criterion for high ozone was that the daily maximum 8-hour ozone concentration in a region was higher than 80 ppb. The 80 ppb cutoff is shown as a red horizontal line in Figure 1-1. For each region, we examined periods of observed high 8-hour ozone concentrations in order determine whether the possibility exists that modeled winds may have been degraded by the presence of downdrafts from anomalous or overly intense convection in MM5.

For each day on which high ozone occurred and precipitation was present over the domain, we compared the observed and modeled daily total precipitation on the 12 km and 4 km grids to determine whether there were localized areas where rainfall was overestimated. The presence of localized maxima in the modeled fields that do not appear in the CPC field suggests that there may have been anomalous modeled convection on that day. On days when anomalous convection may have occurred, we reviewed that day's wind speed and direction time series for each region to determine whether the wind time series showed anomalous shifts in wind speed and direction. Hourly modeled precipitation fields were reviewed for the presence of intense, localized rainfall occurring at a time and place when it may have influenced the anomalous wind shifts. We supplemented this analysis with comparison of late afternoon visible satellite imagery with hourly modeled rainfall totals. Visible satellite images from the GOES-12 satellite were provided by TCEQ along with MODIS visible images downloaded from the Space Science and Engineering Center at the University of Wisconsin-Madison (http://eosdb.ssec.wisc.edu/modisdirect/). For the period June 9-July 3, GOES-12 2315Z images were available, and for the period May 29-June 8, MODIS images from various times of day were used.

Comparison of modeled precipitation fields with satellite images provides a snapshot of the model's correspondence with the observed cloud field, and shows regions where anomalous modeled convection may be present. Because it is impossible to tell from satellite imagery whether it is raining at a given location, this analysis serves as a gross error check on the model performance and suggests times when further analysis would be appropriate. For example, if the model predicts a localized rainfall maximum of several cm in a region where there is no cloud cover in the satellite photo, it suggests that anomalous convection may be present. Without hourly rainfall observations, it is difficult to assess whether the MM5 precipitation field at a given hour shows the presence of anomalous convection, but the analysis described above will serve as a screening tool that will suggest whether future sensitivity tests to cumulus parameterization choice are indicated. In Section 5, we will review each of the four regions in turn, evaluating each high ozone day in each region.

Dallas-Fort Worth

The Dallas-Fort Worth area experienced a high 8-hour ozone episode from June 3-15, but by June 3, little precipitation was occurring in Northern Texas. The wind performance during this episode was generally good. Although there is anomalous convection in the model during this period, it does not have a significant adverse impact on the DFW region average modeled winds. There is a wind direction shift on June 8 that appears in the model fields but not in the observations (Figure 3-8); however, there is no rain in the area on that day, and this wind direction shift is unrelated to anomalous convection.

On June 18, the Dallas-Forth Worth area exceeded the 8-hour ozone standard. The CPC precipitation field shows a maximum southeast of DFW (Figure 4-6). On the 12 km grid, MM5 replicates the location of the precipitation maximum reasonably well, and does reproduce some of the banded structure seen in the observations. The model is too dry in northern Texas, and overpredicts rainfall in northeast Texas. On the 4 km grid, the model locates the precipitation maxima too far to the southeast, underestimates the intensity of the northern band of observed precipitation, and is too dry in northern Texas. Figure 5-1 shows hourly precipitation totals for an hour on the morning of the June 18. During the morning of June 18, there were periods of locally intense rainfall to the south of the DFW area on the 12 km grid in the region where the observations show the occurrence of precipitation on this day. On the 4 km grid, the precipitation occurs further south, with most rain falling near the coast. The winds (Figure 5-1, Figure 3-8) show a direction shift that appears in the 12 km grid time series, although it is exaggerated; the wind shift is better simulated on the 4 km grid. It is possible that the model's difficulty with this wind shift on the 12 km grid was influenced by the presence of overly intense or mistimed convection, which was present on the morning of June 18 to the south of DFW.

The satellite photo for 2315Z on June 18 (Figure 5-2) was taken well after the wind shift described above, and shows reasonable correspondence with the 12 km MM5 rainfall field. The satellite image shows possible rain activity near the Louisiana-Texas border at this time, and MM5 does locate rainfall in this vicinity. The satellite image shows a trail of clouds arcing southwestward across Texas, and the modeled fields show rainfall in this approximate pattern. There is dramatically less rainfall on the 4 km grid however, which shows less correspondence with the satellite image, and does not indicate anomalous convection.

Dallas-Fort Worth had another episode of elevated 8-hour ozone levels on June 27-July 1. On June 27-July 1, there is little or no rain in northern Texas (Figure 4-9). For the Dallas-Fort Worth area, the model wind performance is not likely to have been significantly affected by the presence of anomalous thunderstorm activity during this period.

San Antonio

The San Antonio area had high 8-hour ozone concentrations on June 8, June 13-14, and June 27-29. On June 8, there was little rain over Texas on either the 4 km or 12 km grid (Figure 4-4). Anomalous thunderstorm activity did not play a role in wind performance in San Antonio on June 8.

On June 13, the hourly 4 km grid MM5 precipitation field shows a band of regions of intense localized rainfall moving southwestward across the domain starting in the TLM area around midnight on June 13 and arriving in the San Antonio/Austin area by 8 pm that evening (not shown). Figure 5-3 shows the modeled precipitation fields and the visible satellite image taken at 2315Z. The satellite image suggests that, at this time, there may be anomalous convection on the 4 km grid. The satellite image shows some evidence of convective activity in the Houston area, and the 4 km grid simulation captures some of this, but extends the convection too far to the north and west. On the 12 km grid, the model shows light precipitation in a region of the satellite photo that is partly cloudy.

At 5 pm on June 13, the observed and modeled San Antonio wind direction time series for both the 4 km and 12 km grids (Figure 5-4) diverge and do not correspond well again until early in the morning of June 14. Wind speed is overestimated on both the 12 km and 4 km grids during the afternoon of June 13 (Figure 3-5). The 4 km grid simulates the observed reduction in wind speed more accurately, although there is a peak at 7 pm in the 4 km wind speed time series that does not appear in the observations. By the time of the 2315Z satellite photo (Figure 5-5), the overall pattern of the model precipitation fields corresponds fairly well to the observed cloud fields. On the 4 km grid, it is possible that MM5 overestimates the intensity of convection in some cells in the Victoria area, but lack of rainfall observations with greater temporal resolution than one day prevents a definitive answer. On both June 13 and June 14, hourly modeled rainfall fields show there is convection on the 4 km grid in the San Antonio area (not shown), and Figures 5-3 and 5-5 suggest that there may be anomalous convection in the area on June 13-14. It is certainly possible that the wind field errors on the 4 km were influenced in part by the presence of anomalous convection. However, the wind direction time series on the 12 km grid is very similar to that of the 4 km grid and the wind speed time series on the 4 km grid is arguably a better representation of the observed time series; this suggests that other factors played a role in determining the character of the modeled time series.

During the June 27-29 high ozone period, there was no strong precipitation in the model indicating the presence of thunderstorms in MM5 during this time (Figure 4-9).

Austin

The Austin area had high 8-hour ozone concentrations on June 8, and again on June 29-30. On June 8, the model predicted little rain in Texas and there was no evidence of anomalous convection near Austin.

On June 29, the 4 km and 12 km grids show little rainfall over land. There is a rainfall maximum over the Gulf of Mexico on the 4 km grid, but it is not possible to assess whether it is anomalous using the CPC dataset. On June 30, the observations show rain near southern coastal Texas (Figure 4-9), but the model predictions correspond well to the observed field, showing no evidence of anomalous convection.

Tyler-Longview-Marshall

Figures 1-1 and 1-2 show that high 8-hour ozone values were recorded in the TLM region ozone on June 7, June 12, June 14, and June 30. On June 7, the CPC daily total observations show a band of precipitation oriented northwest-southeast and lying roughly along the Texas-Louisiana and Oklahoma/Arkansas borders (Figure 4-4). The daily total precipitation maximum lies along the intersection of the Texas, Louisiana, and Arkansas borders. On the 12 km grid, the model locates the maximum slightly south of the observed location, and shows two local maxima rather than a single maximum, as in the observations. On the 4 km grid, the maximum is concentrated into a smaller area, and is more intense (126 mm) than the maxima on the 12 km grid (58 mm) or in the observations (46 mm). On the 4 km grid, the model locates the maximum southeast of its location in the observations, and the overall pattern shows too much precipitation in southeastern Louisiana and too little over Oklahoma and Arkansas.

Examination of the hourly precipitation totals from MM5 indicates that at midnight on June 7, there is rainfall in Northeast Texas along the Texas-Louisiana border. It remains intense until about 8 am and then begins to lessen (Figure 5-6). By noon, precipitation is nearly absent from the modeled fields. Figure 3-7 shows that in the early morning hours of June 7, the wind speed on the 4 km and 12 km grids is higher than observed, and does not begin to match the observations well until about 9 am. The model misses a wind shift that appears at 9 am in the observations (Figure 5-6). Because of the timing and intensity of the precipitation in MM5, it is possible that misplaced or over predicted convective activity contributed to the poor wind performance on June 7. This is a day when the observations showed a fairly diffuse rainfall pattern, but the model tended to concentrate the rainfall across a smaller area, and to make it more intense, particularly on the 4 km grid.

Figure 5-7 shows the visible satellite image taken at 2315Z. At this time, there is fairly good correspondence between the observed and modeled wind speed and direction. There is reasonably good agreement between the 12 km grid rainfall field for this hour and the location of clouds in the satellite image, with the modeled rain fields reflecting the fact that the rain event in TLM earlier in the day has ended. The 4 km grid shows possible thunderstorm activity in central Louisiana, but is nearly dry over Texas.

On June 12, the observed daily total precipitation fields suggest that there should be little or no rainfall in the TLM area or in Louisiana (Figure 5-8). The model shows some rain along the Gulf Coast and also late on the night of June 12 in Northern Louisiana. The maximum modeled rainfall was 26 mm near the intersection of the Texas, Arkansas, and Louisiana borders during the 11 pm hour. MM5 has difficulty in simulating the winds on both grids on this day (Figure 5-9). Between midnight and 6 pm, the observations show three wind shifts. On the 12 km grid, the model shows the first two shifts in wind direction, although there is a phase delay, but misses the third wind shift. On the 4 km grid, the model misses the first wind shift, is early on the second wind shift, and completely misses the third. Since all three wind shifts occur before 2 pm, it is unlikely that the wind error was caused by downdrafts from the anomalous storms in Louisiana, which did not organize and strengthen until approximately 7 pm.

At the time of the 2315Z satellite image (Figure 5-10), there appears to be thunderstorm activity along the Arkansas-Louisiana border and in southeastern Louisiana. On the 12 km grid, the model picks up this activity, showing intense localized rainfall in southeastern Louisiana. On

both the 4 km and 12 km grids, there is weak rainfall in southern Arkansas. The satellite image indicates strong convective towers in this region, so the model may be understating or mistiming convective activity there.

On June 14, the observations show precipitation occurring in the Houston area (Figure 4-5). On the 12 km grid, this area of rain is located well to the southwest of Houston, and has a banded structure that does not correspond well with the observations. The pattern on the 4 km grid is closer to the observations, but the maximum is nearly an order of magnitude too intense, and the rain is located too far to the west. As discussed above, the 4 km grid showed regions of convection moving southeast of the TLM area on the night of June 13.

Modeled wind speeds in TLM were too high on both grids during the night of June 13 and the morning of June 14, with performance improving during the middle of the day on June 14 and then becoming too fast again during the evening of June 14 (Figure 3-7). There is a shift in the observed wind field beginning at 1 am (Figure 5-9). This wind shift is delayed but does occur (twice) on the 12 km grid, however the wind shift is absent from the 4 km wind field. The 4 km grid does show some localized rainfall immediately to the southeast of the TLM area on the evening of June 13 (Figure 5-3). It is possible this mischaracterized precipitation affected the 4 km wind field, causing it to miss the observed wind direction excursion. However, the 12 km wind field also had difficulty simulating this wind shift, and its rainfall maximum is an order of magnitude less intense and located further to the southeast.

On June 30, there was no precipitation in the TLM area, and wind performance on this day was not affected by the presence of anomalous thunderstorms.

Summary

- Anomalous convection was noted intermittently throughout the simulation, and did occur on some of the high 8-hour ozone days during the episode.
- Although anomalous convection may have played a role in degrading performance on several of the high ozone days, it is unlikely to be the only factor.

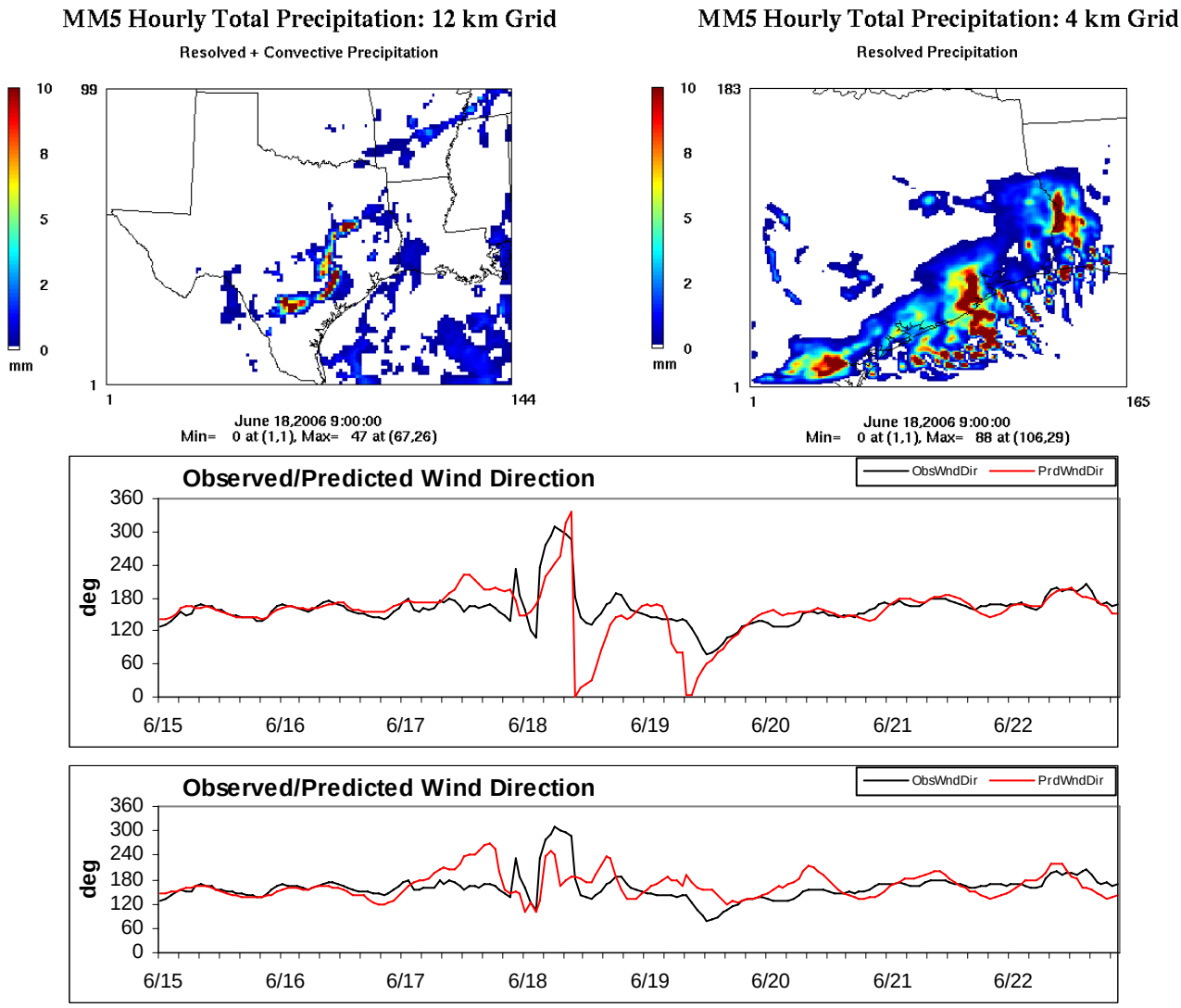

Figure 5-1. June 18, DFW. Upper left hand panel: MM5 hourly total precipitation (mm) on the 12 km grid. Upper right hand panel: MM5 hourly total precipitation (mm) on the 4 km grid. Upper center panel: observed (black) and predicted (red) wind direction time series for the DFW area on the 12 km grid. Lower center panel: observed (black) and predicted (red) wind direction time series for the DFW area on the 4 km grid.

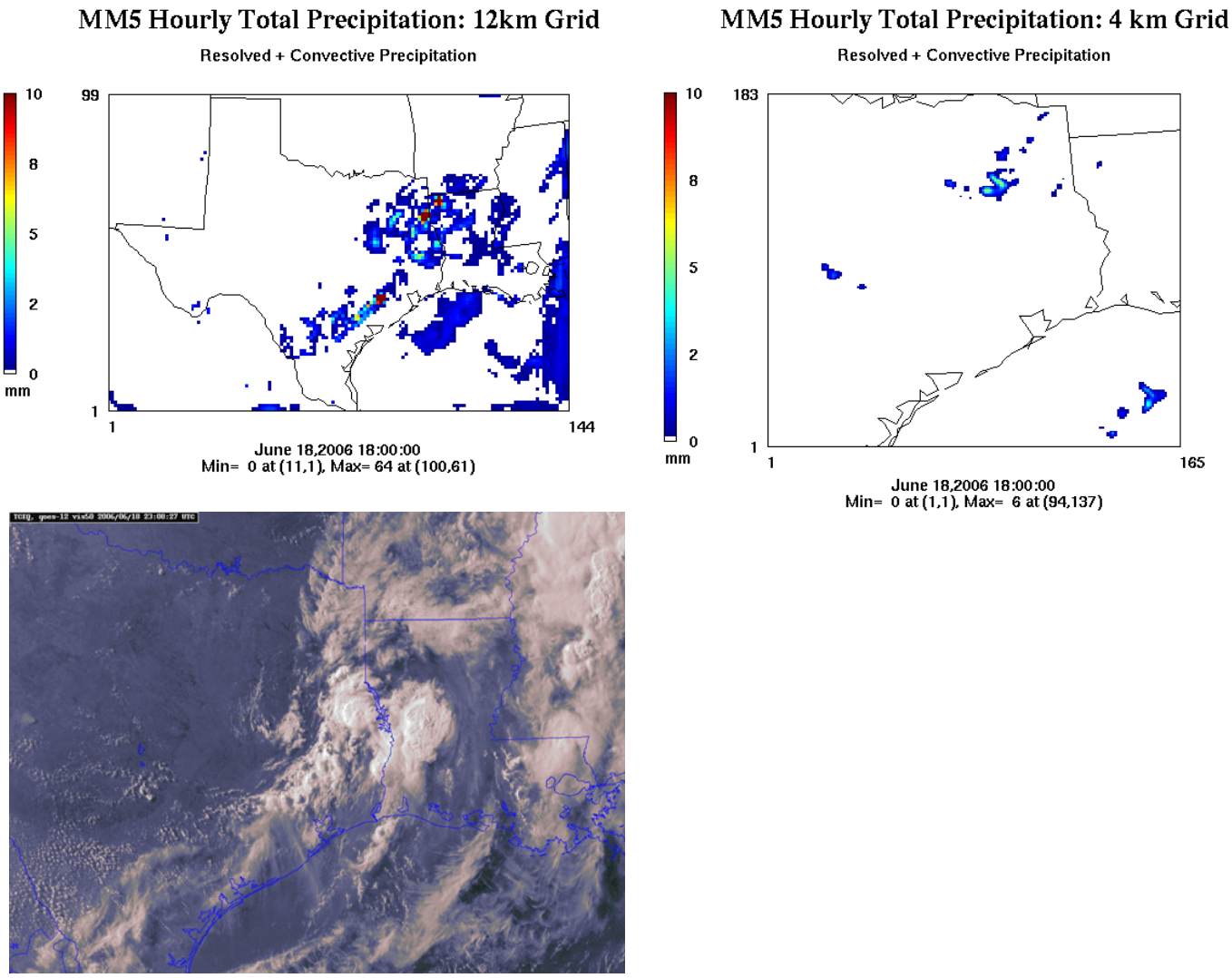

Figure 5-2. DFW, June 18. Upper left hand panel: MM5 12 km grid precipitation for the hour 1800 CDT. Upper right hand panel: MM5 4 km grid precipitation for the hour 1800 CDT. Lower left hand panel: GOES-12 visible satellite image from 2315 Z (1815 CDT) on June 18.

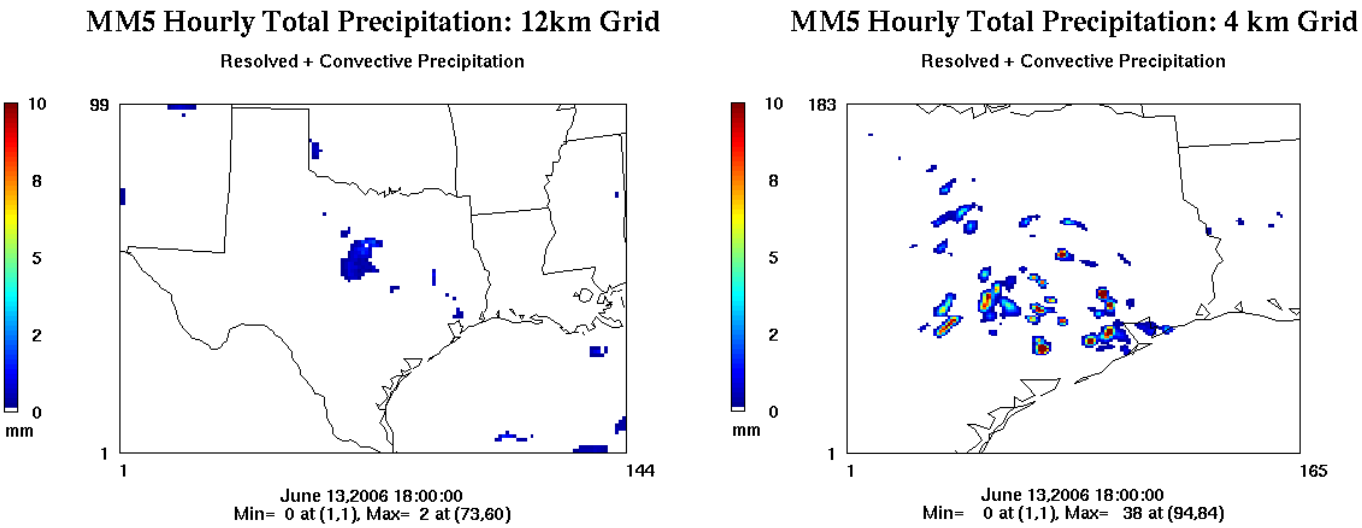

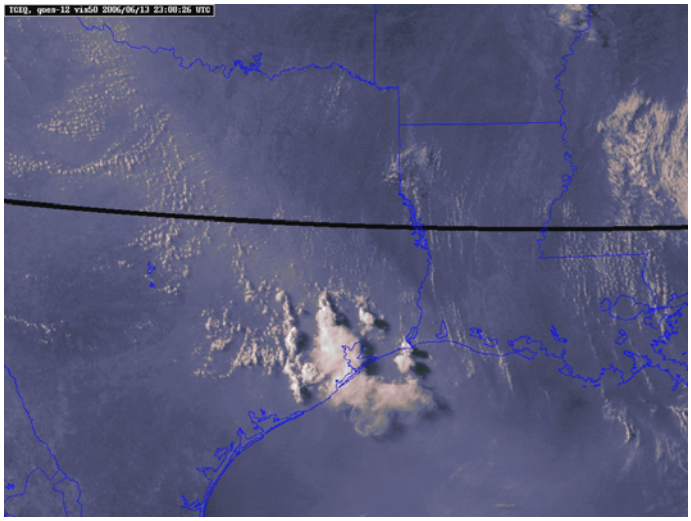

Figure 5-3. San Antonio, June 13. Upper left hand panel: MM5 12 km grid precipitation for the hour 1800 CDT. Upper right hand panel: MM5 4 km grid precipitation for the hour 1800 CDT. GOES-12 visible satellite image from 2315 Z (1815 CDT) on June 13.

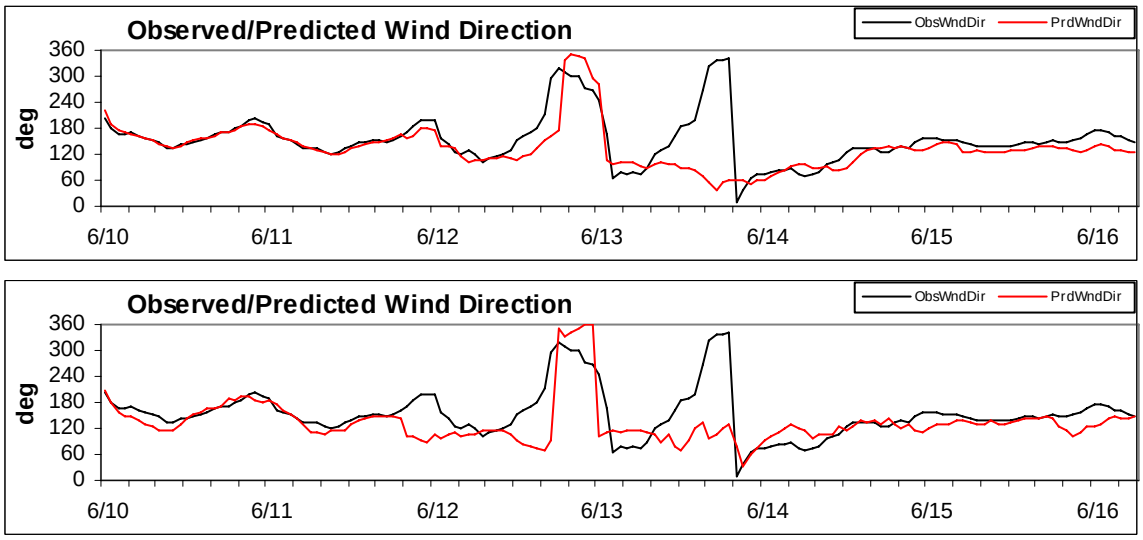

Figure 5-4. June 13-14, San Antonio. Upper panel: observed (black) and predicted (red) wind direction time series for the San Antonio area on the 12 km grid. Lower center panel: observed (black) and predicted (red) wind direction time series for the San Antonio area on the 4 km grid.

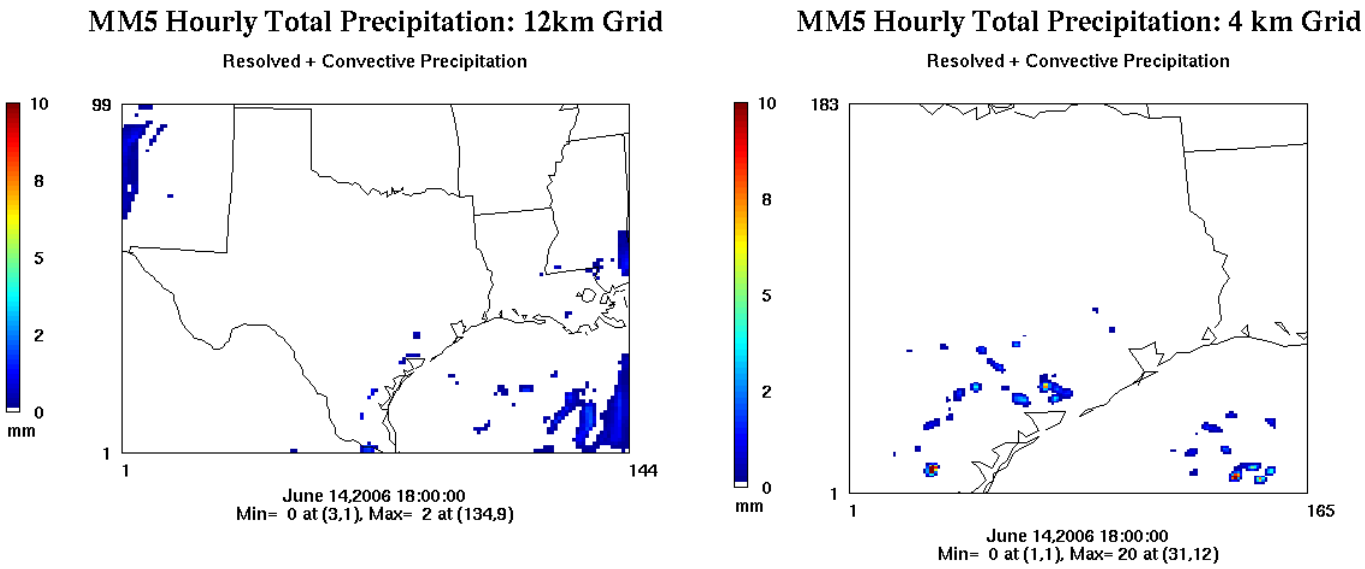

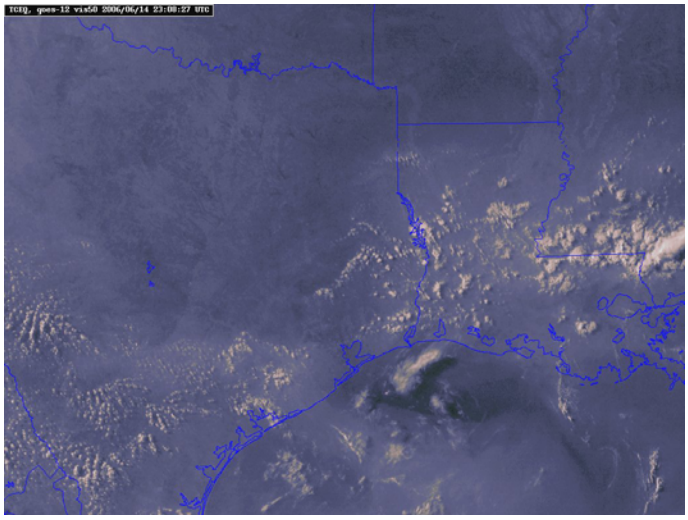

Figure 5-5. June 14. Upper right hand panel: MM5 12 km grid precipitation for the hour 1800 CDT. Upper left hand panel: MM5 4 km grid precipitation for the hour 1800 CDT. Visible satellite image from 2315 Z (1815 CDT) on June 14.

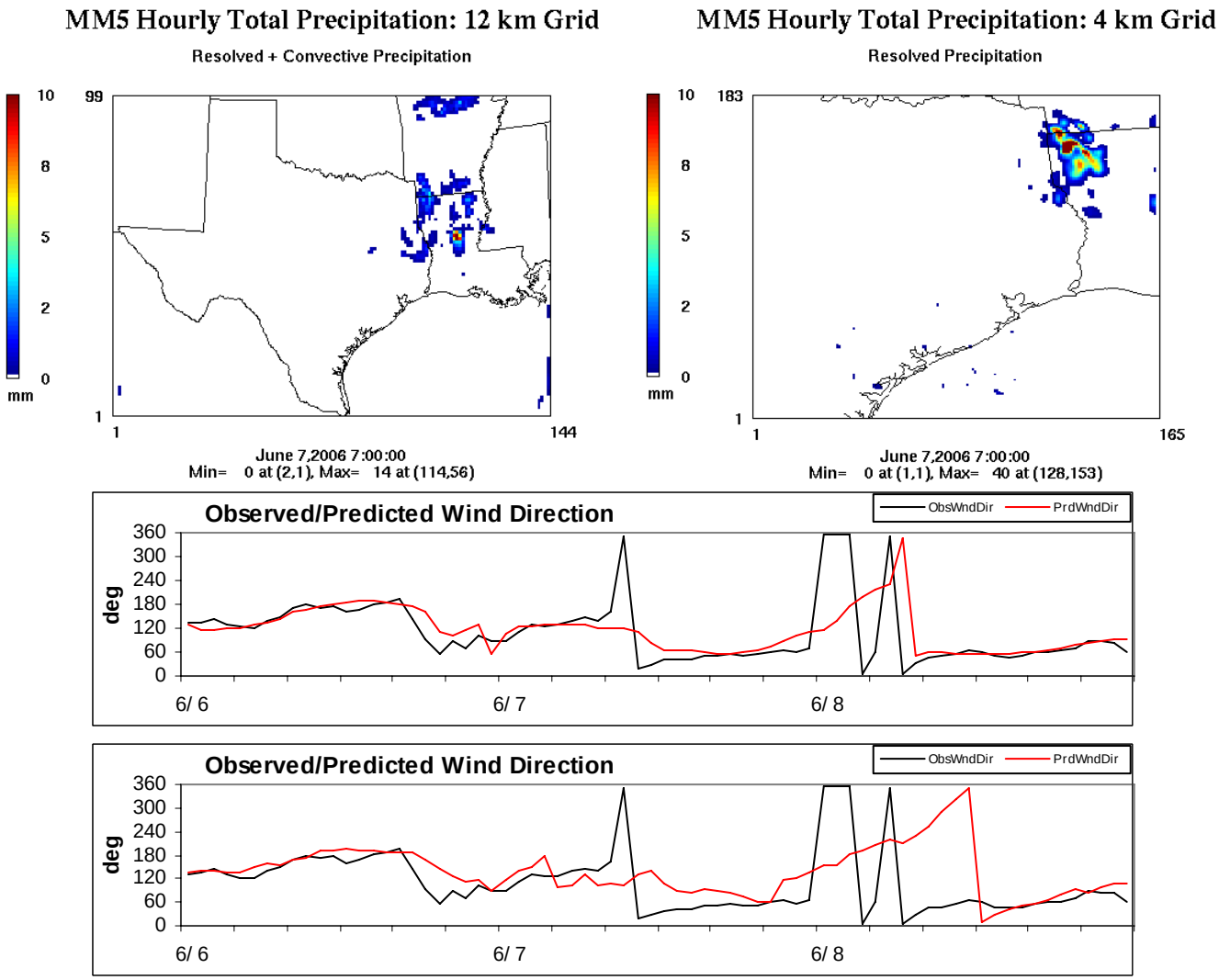

Figure 5-6. June 7, TLM. Upper left hand panel: MM5 hourly total precipitation (mm) on the 12 km grid. Upper right hand panel: MM5 hourly total precipitation (mm) on the 4 km grid. Upper center panel: observed (black) and predicted (red) wind direction time series for the TLM area on the 12 km grid. Lower center panel: observed (black) and predicted (red) wind direction time series for the TLM area on the 4 km grid.

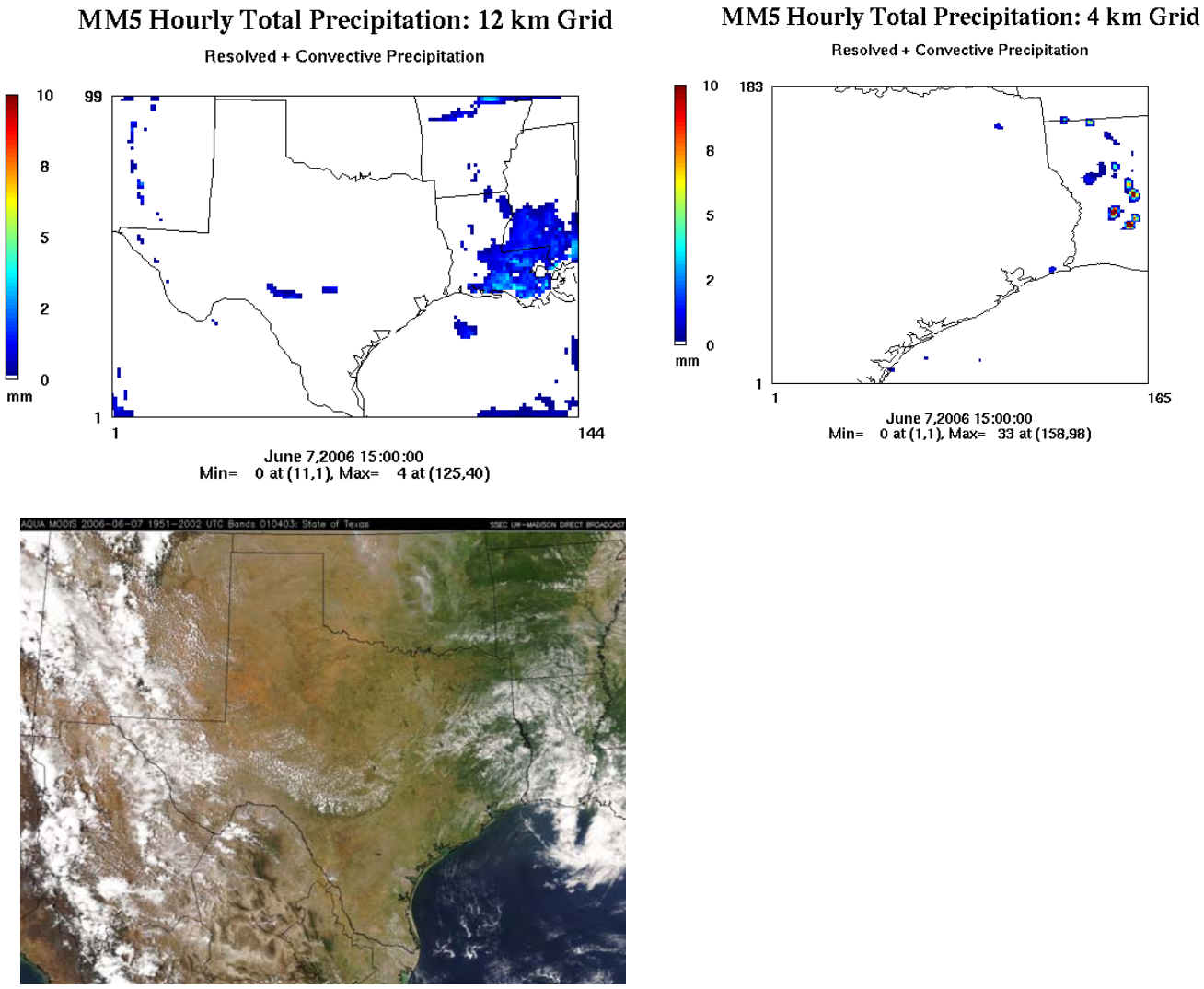

Figure 5-7. June 7, TLM. Upper right hand panel: MM5 12 km grid precipitation for the hour 1500 CDT. Upper left hand panel: MM5 4 km grid precipitation for the hour 1500 CDT. MODIS AQUA visible satellite image from 1951-2002 Z (1451-1502 CDT) on June 7.

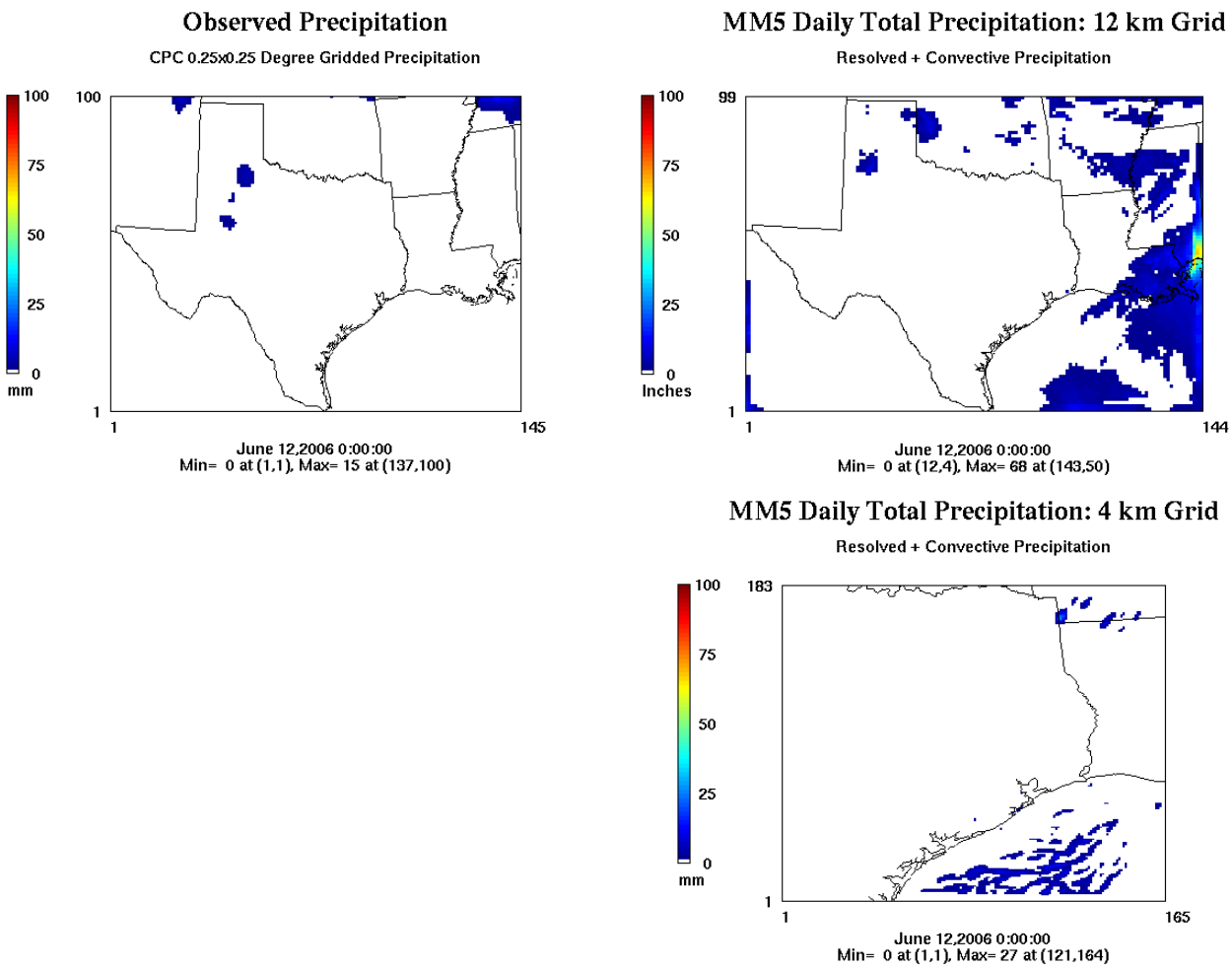

Figure 5-8. June 12, TLM. Upper left hand panel: CPC observed daily precipitation total (mm). Upper right hand panel: MM5 daily precipitation total (mm) on the 12 km grid. Lower right hand panel: MM5 daily precipitation total (mm) on the 4 km grid.

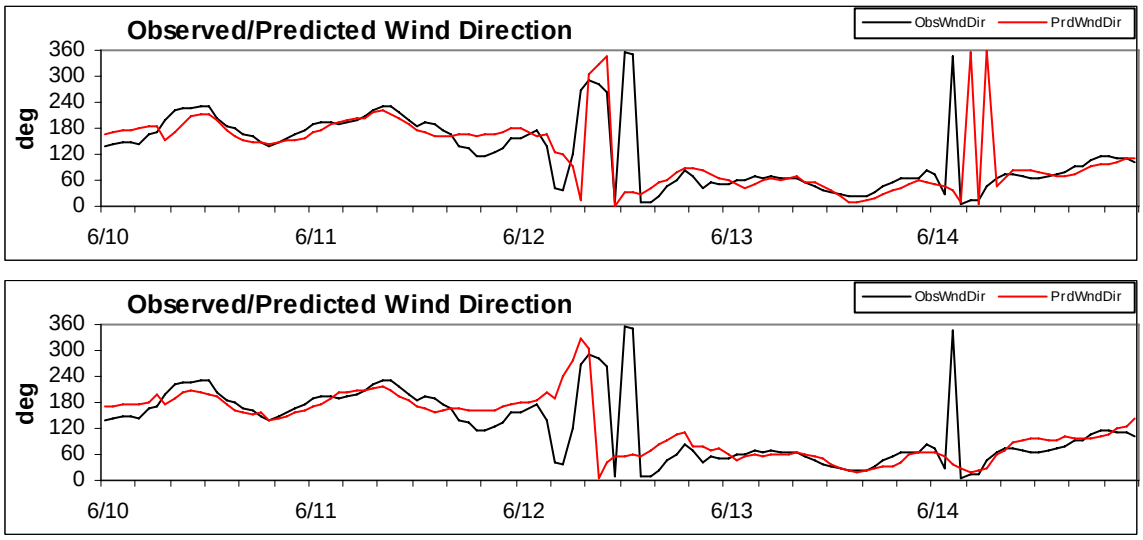

Figure 5-9. June 12 and June 14. Observed (black) and predicted (red) wind direction time series for the TLM area on the 12 km grid. Lower center panel: observed (black) and predicted (red) wind direction time series for the TLM area on the 4 km grid.

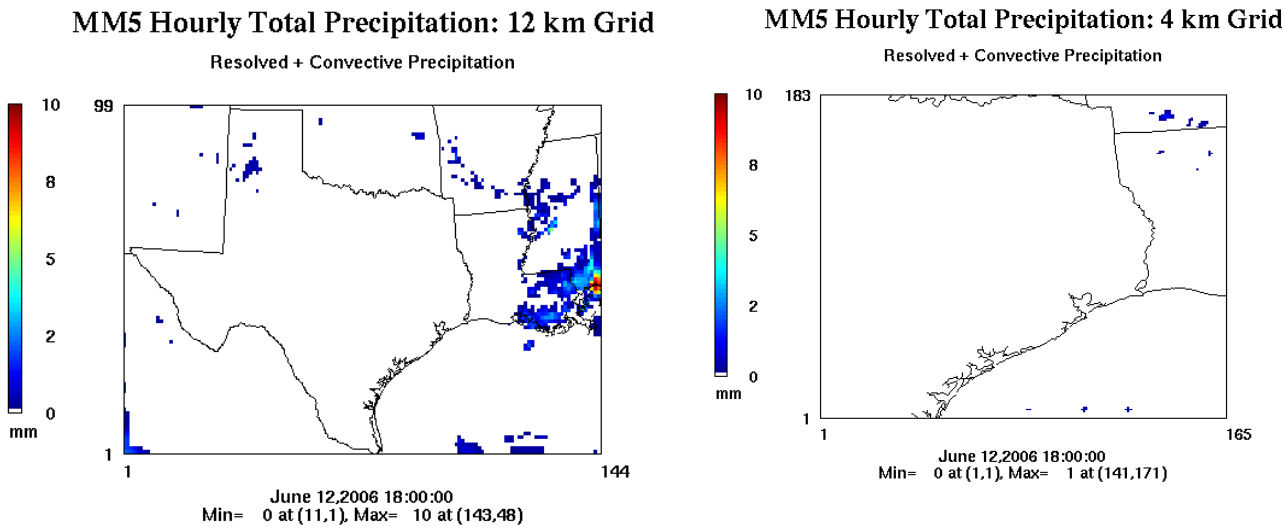

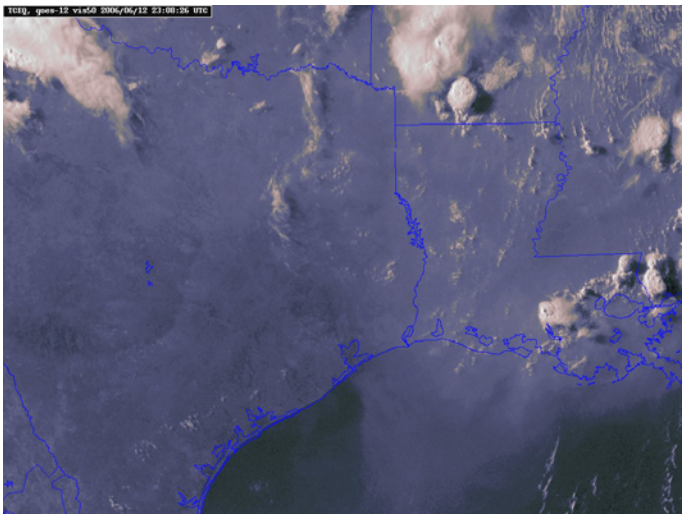

Figure 5-10. June 12, TLM. Upper right hand panel: MM5 12 km grid precipitation for the hour 1800 CDT. Upper left hand panel: MM5 4 km grid precipitation for the hour 1800 CDT. GOES-12 visible satellite image from 2315 Z (1815 CDT) on June 12.

6. SUMMARY

Here follows a summary of MM5 performance in the initial modeling of the May 29-July 3, 2006 extended Texas ozone episode:

Comparison of Performance on 12 km versus 4 km Grids

- Model surface performance degraded for both wind speed and wind direction on the 4 km grid relative to the 12 km grid.
- Model surface performance improved for temperature and humidity on the 4 km grid relative to the 12 km grid.
- Precipitation on the 4 km grid tends to be confined to smaller areas and to have higher maxima, while precipitation tends to occur over a larger area on the 12 km grid, and to have lower maxima.
- Observed daily precipitation totals were not well simulated by the model on either the 12 km or the 4 km grid.
- The observed episode total precipitation pattern over Texas was reproduced with greater fidelity on the 4 km grid than on the 12 km grid.

Surface Wind Performance

- On both the 4 km and 12 km grids, MM5 met the performance benchmark for wind speed for all four regions (Dallas-Fort Worth, San Antonio, Austin, and Tyler-Longview-Marshall).
- The wind direction performance met the benchmark on the 12 km grid for Dallas-Fort Worth, but not for San Antonio, Austin, or Tyler-Longview-Marshall.

Surface Humidity Performance

- Model performance was within the benchmark for humidity on the 4 km and 12 km grids for all four regions.
- On the 12 km grid, the model showed a wet bias, and this wet bias was reduced for all regions in going to the 4 km grid.
- The reduction in wet bias was due to better simulation of the daily minima in humidity in the 4 km run. On the 12 km grid, the model remained too wet during the minima.

Surface Temperature Performance

- Temperature performance showed a general cold bias.
- On the 12 km grid, only San Antonio was within the benchmark for temperature bias, and all four regions failed to meet the temperature error benchmark.
- On the 4 km grid, temperature performance improved so that all regions but TLM met the benchmark for bias. All four regions remained outside the benchmark for error on the 4 km grid.

Assessment of Anomalous Convection

- Anomalous convection was present during many days of the simulation, but occurred on only a small number of high ozone days. On a subset of these high ozone days, anomalous convection may have degraded the wind performance, but was unlikely to have been the only contributing factor.

This initial MM5 run can serve as a good starting point for the development of a meteorological database for future ozone modeling of the May 29-July 3, 2006 episode. The performance of the initial run was encouraging, but further work should be undertaken to improve the surface performance so that the model meets most performance benchmarks and to reduce the incidence of anomalous convection throughout the simulation, and particularly on high ozone days. A primary goal is to improve the wind direction performance. Good wind performance is essential if future ozone modeling efforts are to succeed. We recommend sensitivity testing designed to address the issues noted above and to optimize model performance over the San Antonio/Austin and Dallas/Tyler-Longview-Marshall areas. Below, we provide a list of recommendations for further work, ordered by the sequence in which they should be carried out.

Recommendations for Further Work

1. 3D analysis nudging of temperature on the 12 km grid should be turned on in all future simulations.

2. Comparison of the ds472 and CAMS datasets should be undertaken to understand differences in surface winds, temperature and humidity.

3. Additional nudging may improve the wind performance. We propose nudging to ds472 surface wind observations on both the 12 km and 4 km grids. CAMS data will be held in reserve for model evaluation.

4. Additional nudging of winds should be performed using TEXAQS II profiler data as this data becomes available.

5. A comparison of the predicted PBL heights and comparison with TEXAQS II profiler data should be undertaken. This will help determine whether sensitivity tests using different MM5 PBL/land surface schemes are indicated. This task will require development of a new software tool to average MM5 output PBL heights over several grid cells surrounding the profiler and generate a time series of model PBL heights which may be compared with the observed mixed layer heights from the profiler.

6. Anomalous convective activity may have had an adverse impact on model performance during several high ozone days. Although it is unlikely to have been the only contributing factor degrading performance on those days, it is desirable to reduce the amount of anomalous convection. There is no obvious method for accomplishing this goal. Guidance from the developers of MM5 is that on grid scales of 4 km, convection should not be parameterized. On the 12 km grid, however, parameterization is necessary because the model cannot resolve the updraft and downdrafts components of a storm. We recommend a sensitivity test in which the Grell cumulus scheme is replaced with the Kain-Fritsch II

cumulus scheme. The Kain-Fritsch II scheme incorporates a parameterization of shallow convection, and has been shown to perform reasonably well under a variety of meteorological conditions. This test could be run over the first two weeks of the simulation, which contains periods of both rainy and dry weather.

7. For evaluation of the precipitation fields on 4 km grid, observed rainfall data at a spatial resolution greater than that of the CPC data set is highly desirable. The National Weather Service National Precipitation Analysis data set contains gridded observations of precipitation at 4 km resolution (http://www.srh.noaa.gov/rfcshare/precip_analysis_new.php). This dataset is derived from rain gauge and radar observations, and contains daily average observations where the day is defined to begin and end at 12Z. We recommend that this dataset be processed into a convenient format for evaluation of future sensitivity testing, which means that it must be projected onto the LCP modeling grid and that daily averages beginning and ending at 0Z be formed in order to make it compatible with MM5 output.

Acknowledgements

Satellite images were provided by Ben Coughran of TCEQ. CAMS data in METSTAT-ready format for the surface evaluation were provided by Doug Boyer of TCEQ.

ENVIRON thanks Doug Boyer and Bright Dornblaser of TCEQ, who graciously made available software they developed for integrating wind profiler observations into MM5 nudging files.

The NPN profiler data was supplied by NOAA's Earth System Research Laboratory Global Systems Division.

REFERENCES

Emery, C.A. and E. Tai. 2001. "Enhanced meteorological modeling and performance evaluation for two Texas ozone episodes." Prepared for the Texas Natural Resource Conservation Commission, by ENVIRON International Corporation.

Kemball-Cook, S., Y. Jia, C. Emery, R. Morris, Z. Wang and G. Tonnesen. 2004. Draft Protocol: 2002 Annual MM5 Simulations to Support WRAP CMAQ Visibility Modeling for the Section 308 SIP/TIP. Western Regional Air Partnership, Regional Modeling Center. December 10. http://pah.cert.ucr.edu/aqm/308/docs/WRAP_modeling_protocol1.pdf

Molinari, J., 1993. An overview of cumulus parameterization in mesoscale models. *The Representation of Cumulus Convection in Numerical Models*. K. Emanuel and D. Raymond, Ed. American Meteorological Society, p.155-159.

Molinari, J. and M. Dudek, 1992: Parameterization of convective precipitation in mesoscale numerical models. *Mon. Wea. Rev*., **120**, 326-344.

PSU/NCAR, 2005. PSU/NCAR Mesoscale Modeling System Tutorial Class Notes and User's Guide: MM5 Modeling System Version 3. http://www.mmm.ucar.edu/mm5/On-Line-Tutorial/presentations/tut-presentations.html.

Tesche, T.W. et al. 2002. "Operational Evaluation of the MM5 Meteorological Model over the Continental United States: Protocol for Annual and Episodic Evaluation." Prepared for the U.S. Environmental Protection Agency, Office of Air Quality Planning and Standards, prepared by Alpine Geophysics, LLC, Ft. Wright, KY.